H-INFINITY OPTIMAL CONTROL OF ACTIVE DUMPERS FOR AUTOMOTIVE SUSPENSION SYSTEMS AND CIVIL STRUCTURES

by

Jamal Ezzine

A dissertation submitted to the faculty of Modelling for Engineering

University of Calabria

in partial fulfilment of the requirements for the degree of

Doctor of Philosophy

International Doctorate Programme

Bernardino Telesio School of Hard Sciences

University of Calabria

November 2009

Copyright © 2009 Jamal Ezzine

All Rights Reserved

University of Calabria

DEPARTMENT APPROVAL

of a dissertation submitted by

Jamal Ezzine

This thesis has been reviewed by the research advisor and research coordinator, and has been found to be satisfactory.

Date	Prof. A. Casavola and Prof. A. Vulcano, Advisor
Date	Prof. M. Aristodemo, Research Coordinator

ABSTRACT

H-INFINITY OPTIMAL CONTROL OF ACTIVE DUMPERS FOR AUTOMOTIVE SUSPENSION SYSTEMS AND CIVIL STRUCTURES

Jamal Ezzine

Department of modelling for engineering

Doctor of Philosophy

In recent years the protection of structures against hazardous vibration has gained special interest. Structures such as buildings, bridges and vehicles are subject to vibrations that may cause malfunctioning, un-comfort or collapse. It is an extended practice to install damping devices in order to mitigate such vibrations. Furthermore, when the dampers are controllable, the structure acts as an adaptronic system. Adaptronic systems are characterized by their ability to respond to external loading conditions and adapt themselves to these changes. These abilities can be exploited to solve the vibration mitigation problems through the installation of controllable dampers and the design of appropriate control laws for an adequate actuation. These modern systems in the case of vehicle suspension systems offer improved comfort and road holding in varying driving and loading conditions compared to traditional passive devices.

ACKNOWLEDGMENTS

I would like to express my sincere gratitude to Prof. M. Aristodemo, Prof. A. Casavola and Prof. A. Vulcano who has guided me through out my research activity.

Contents

Table of Contents **vi**

List of Figures **ix**

1 Introduction **1**
1.1 Overview 1
1.2 Problem Definition 1
1.3 The Scope of the Thesis 2
1.4 Structure of the Thesis 3

2 Vehicle Modelling and Dynamics **4**
2.1 Introduction 4
2.2 Vehicle Ride Model 5
2.2.1 Vehicle Degrees's of Freedom (DOF) 6
2.2.2 Types of Suspensions Control System 9
2.3 MR Damper and Parameters Estimation 10
2.3.1 Design of Magneto-rheological Damper 10
2.3.2 Experimental Results 11
2.3.3 Applications of MR Technology in the Industry 13
2.4 Vehicle Motion 15
2.5 Tyre Modelling 16
2.6 Road Modelling 17
2.7 Simple Car Model 20
2.7.1 Quarter-Car Model 21
2.7.2 Half Car Model 23
2.8 Human Body Response 25
2.8.1 Low-frequency Seated Human Model 26
2.8.2 Multy Frequency Input 27
2.9 Passenger Car Model 29
2.9.1 Quarter Car Passenger Model 29
2.9.2 Half Car Passenger Model 31

3 Controller Design **36**
3.1 Control Algorithm . . . 36
3.1.1 Optimal Control . . . 36
3.1.2 Predictive Control . . . 40
3.1.3 Robust Control . . . 42
3.2 H_∞ Theory . . . 45
3.2.1 Statement of H_∞ Control . . . 46
3.2.2 Specifications with Mixed Sensitivity Functions . . . 51
3.3 LMI based Hinf Control Suspensions Car . . . 55
3.3.1 Example Linear Matrix Inequality . . . 55
3.3.2 Some Standard LMI Problems . . . 56
3.3.3 Problem LMI based Hinf Problem . . . 58

4 Simulations Result **61**
4.1 Results of simple car model . . . 61
4.1.1 Functions of Weight . . . 61
4.1.2 Results of simple car model . . . 62
4.2 Results of Quarter-Car Model with Passenger . . . 64
4.2.1 Frequency Domain . . . 64
4.2.2 Time domain . . . 64
4.3 Results of Half-car model with passenger . . . 66
4.3.1 Frequency Domain . . . 66
4.3.2 Time domain . . . 69

5 Structural Control in Civil Engineering **70**
5.1 Introduction . . . 70
5.2 Classification of Building Control . . . 71
5.2.1 Passive Control . . . 72
5.2.2 Active Control . . . 73
5.2.3 Semi-Active Control . . . 74
5.2.4 Hybrid Control . . . 75
5.3 Actuator Systems for Active and Semi-Active Building Control . . . 75
5.3.1 Hydraulic Actuation and Active Bracing . . . 75
5.3.2 Hydraulic Actuation and Active Tendons . . . 77
5.3.3 Hydraulic Actuation and the Active Mass Driver . . . 78
5.4 Controllable Fluid Damper . . . 79
5.4.1 Magneto-Rheological Damper Behaviour . . . 80

6 Benchmark Civil Structural Control Problems **85**
6.1 Active Control Systems: The LQG Approach . . . 88
6.2 Semi-Active Control Systems: The Clipped Optimal Control Approach 89
6.3 Three-Story Building . . . 91
6.3.1 Active Bracing System . . . 91

7 Conclusions and Future Work **96**
7.1 Conclusion . . . 96
7.1.1 Automotive Suspension Systems . . . 96
7.1.2 Civil Structures . . . 97
7.2 Future Research Directions . . . 97
7.2.1 Controllable MR Dampers . . . 98
7.2.2 Large-scale Building Problems . . . 98
7.2.3 Nonlinear Building Models . . . 99

A Control Software **100**
A.1 Practical Considerations . . . 101
A.1.1 Time Delay and Time Lag . . . 101
A.1.2 Structural Nonlinearities . . . 102
A.1.3 limited Number of Sensors and Controllers . . . 102
A.1.4 Discrete-Time Control Features . . . 103
A.1.5 Reliability . . . 103

B Hardware Description **105**
B.1 Active Control Force Generation System . . . 106
B.1.1 Control Device Power Supplier . . . 107
B.1.2 Analog Control Console . . . 107
B.1.3 Active Force Generation device (AFGD) . . . 108

Index **110**

Bibliography **110**

List of Figures

2.1 Rear and Front suspension System(*Ricambi Tuning*). 5
2.2 Vehicle Model (for vertical dynamics only). 8
2.3 Magneto-rheological Dampers. 10
2.4 Responses of force under different electric currents 12
2.5 Equivalent damping coefficient vs. velocity 13
2.6 Delphis MagneRide (MR)system 14
2.7 Orientation of Axes. 16
2.8 Spatial Road Profile (model input). 18
2.9 Pseudo-Random Road Profile [GSS$^+$08] 19
2.10 Quarter-car suspension model [KZ06] 22
2.11 Half-car suspension model [KZ06]. 24
2.12 Vehicle and occupant model [GSS$^+$08]. 27
2.13 Quarter-car passenger suspension model [KZ06]. 30
2.14 Half-car passenger suspension model [KZ06]. 32

3.1 The 2 input and 2 output block problem [CAS01] 47
3.2 The DKGF parameterization of all stabilizing compensator [CAS01] 47
3.3 Mixed sensitivity problem as part of H_∞ control problem 53

4.1 Functions of Weighing $(W_{zs}, W_{zu}, W_{zs2}, W_u)$ 62
4.2 QCTF between road profiles y and chassis position x. 63
4.3 QCTF between road profiles y and chassis position $\ddot{x}$. 63
4.4 QCTF between road profiles y and chassis position x. 64
4.5 QCTF between road profiles y and chassis position $\ddot{x}$. 65
4.6 Quarter-car, Responses of passenger positions, in Time Domain . . . 65
4.7 HCTF. between road profiles y_1 and chassis position x. 66
4.8 HCTF between road profiles y_2 and chassis position x. 66
4.9 HCTF between road profiles y_1 and chassis acceleration $\ddot{x}$. 67
4.10 HCTF between road profiles y_2 and chassis acceleration $\ddot{x}$. 67
4.11 HCTF between road profiles y_1 and pitch acceleration $\ddot{\theta}$. 68
4.12 HCTF between road profiles y_2 and pitch acceleration $\ddot{\theta}$. 68
4.13 Half-car, Responses of passenger positions, in the time response . . . 69

5.1 Passive a, Active b, and Semi-Active c 72

5.2 Base isolation schematic 74
5.3 Hydraulic actuation and active tendon configuration. 77
5.4 Tuned Mass-Damper. 78
5.5 Magneto-rheological Dampers 80
5.6 Schematic model of magneto-rheological dampers [SDSC97] 82
5.7 MR force due to a sinusoidal displacement and varying input voltages. 83
5.8 MR force due to a sinusoidal displacement and varying input voltages. 84

6.1 Clipped-Optimal Control Strategy 90
6.2 Three-story building schematic. 92
6.3 With a. b.: displacement of the (a) first, (b) second, and (c) third floors. 93
6.4 With a. b.: acceleration of the (a) first, (b) second, and (c) third floors. 94
6.5 With MR: acceleration of the (a) first, (b) second, and (c) third floors. 95

B.1 General hardware function of the active control system. [CAS01] . . 106
B.2 Active control force generation system(ACFGS) [CAS01]. 108

Chapter 1

Introduction

1.1 Overview

In recent years, designers of modern vehicle suspensions have begun to seriously consider the use of active suspensions due to their potential to improve the ride and road handling quality and better satisfy the structural constraints. Vehicle suspensions also play an important role in protecting chassis and several parts from vibrations and shocks. Their main objectives are the achievement of minimum variations in dynamic tire loads, good isolation of the chassis from vibration and harshness induced by road unevenness and driving manoeuvres and the stabilization of the chassis during manoeuvres. Most of these new systems equip now luxurious cars.

1.2 Problem Definition

Control of mechanical and civil engineering structures is still an open field and novel theoretical and practical developments must be obtained. Nevertheless, thanks to huge technology advances in areas such as sensing, computation and control important

structural control problems have been solved. Thus, actively controlled suspension systems are now becoming implementable also from economic and reliableness points of view. However, some problems still continue to be open and some others have been appeared with the introduction of innovative suspension systems. For example the introduction of semi-active technologies has produced an important novelty in the field because of their low-energy actuation requirements and maintenance costs. However, more complex control problems have results for their slow responses, low control authority and for the presence of highly nonlinear behaviours due to their intrinsic hysteresis. Thus, one of the challenges in suspension control and civil structural control is that of finding adequate control laws that accomplish minimal design specifications such as robustness, reliability, stability, implementability, minimum control effort, but additionally be able to take into account some particular conditions of the suspension and structural systems, such as actuator dynamics, parametric uncertainties, resonance conditions, non-linearities, coupling and limited measurements.

1.3 The Scope of the Thesis

The problem considered in this thesis is the design and the analysis of control strategies for active suspensions in road vehicles, based on H_∞ optimal control theory. The main focus of the study is the improvement of the vibration isolation while driving on a rough terrain. The vibration level is closely related to the discomfort of the driver and passengers. Vehicle suspensions serve several conflicting purposes, in addition to counteracting the body forces resulting from cornering, acceleration, or braking and changes in payload. Suspensions must isolate the passenger compartment from road irregularities. In this thesis, we decided to study the control of vibration on two types of car modes: first, the one which considers the presence of passengers in

the control scenario and second without passengers. In both cases, quarter-car and half-car dynamical models will be considered. Also, the application of active control on civil structures will be investigated.

1.4 Structure of the Thesis

This doctoral thesis is organized in five chapters. The first one includes an introduction, the motivations and the main objectives of the thesis. *Chapter 2* describes the types of vehicle models and dynamic behaviours considered. Quarter-car and half-car models, with and without the dynamic of the passenger bodies, will be fully detailed. Further, H_∞ optimal control is described and its application to our model is presented, which results one instance of a H_∞ mixed sensitivity control problem, in *Chapter 3*. Simulation results on significant tests are therefore presented and used to pointing out the improvement achievable, over passive suspension systems, by the use of active technology in *Chapter 4*. *Chapter 5* presents various structural control problems in Civil Engineering. Finally, *Last Chapter* will conclude this dissertation.

Chapter 2

Vehicle Modelling and Dynamics

In this chapter the model used for the remainder of this thesis will be introduced, along with its equations of motion and the state space formulation. Once the model is established, it is used to investigate vehicle dynamics for various loading cases and disturbances. This investigation provides fundamental justifications for the research presented in this thesis.

2.1 Introduction

Conventional suspension design is inherently complex and consists of a trade-off, see Figure 2.1, primarily between ride quality and road handling. In addition to this compromise, passive suspension system performance deviates greatly as the vehicle mass varies. Active suspension techniques seek to improve both ride and handling over a wide range of operating conditions. However, a new set of compromises must be traded-off, as active suspension systems increase system complexity and the consume of vehicle power. Nonetheless, active suspension control promises a leap in suspension performance over its passive counterpart. In the following sections, background in-

formation on the common vocabulary used, notation and assumptions made in active suspension development is introduced. Then, the current state of the art of models and control techniques used for active suspension control is reviewed.

Figure 2.1 Rear and Front suspension System(*Ricambi Tuning*).

In terms of development of suspension systems, the most relevant factor that leads to degradation of ride quality is the disturbance from the roughness of the road. There are many ways to classify road disturbances, but usually they are divided into two main classes, vibration and shock. Shock is described by a relatively short duration, high intensity event, such as a pothole or speed bump. Vibration is characterized by prolonged, relatively consistent low amplitude excitations, the typical road roughness. Obviously, a suspension system must be able to cope with both types of road conditions, in addition to any handling requirements during turning.

2.2 Vehicle Ride Model

A broad variety of vehicle mathematical models of increasing degree of complexity has been developed over the years by automotive engineers to provide reliable models

for computer-aided automotive design and vehicle performance assessment.

From a purely mathematical standpoint vehicle models can be categorised as distributed models governed by partial differential equations and lumped parameter models governed by ordinary differential equations [GSS+08]. The former are mainly of interest to vehicle design rather than control algorithm design. Distributed models (typically solved numerically with finite-element-based methods) are widely employed in mechanical, thermal, aerodynamic analyses as well as crash-worthiness analyses. For car dynamics (ride and handling) and control studies, lumped parameter models are usually employed. They typically aim to model either ride or handling dynamics or both. In this thesis only lumped parameter models will be considered. A car can be thought as being composed of two main subsystems: the sprung mass (chassis) and the unsprung masses (wheels, axles and linkages), connected via a number of elastic and dissipative elements (suspensions. tyres etc.) and subjected to external inputs coming from the road profile, the steering system and other external disturbances (e.g., wind gust).

2.2.1 Vehicle Degrees's of Freedom (DOF)

The motion of a vehicle with the nonholonomic constraint of the road has six degrees of freedom (6DOF), classified as follows:

- longitudinal translation (forward and backward motion)
- lateral translation (side slip)
- vertical translation (bounce or heave)
- rotation around the longitudinal axis (roll)
- rotation around the transverse axis (pitch)

- rotation around the vertical axis (yaw)

Vehicle ride is essentially concerned with car vertical dynamics bounce, pitch and roll whereas handling is concerned with lateral dynamics (side slip, yaw, roll). Ride models are typically composed of interconnected spring-mass damper systems and defined by a set of ordinary differential equations. The most trivial representation of a vehicle suspension has 1 DOF. In this simple model the chassis (body) is represented by a mass and the suspension unit by a spring and a damper. Tyre mass and stiffness are neglected as well as any cross-coupling dynamics. By incorporating a wheel into the model, a more accurate representation having 2 DOF (typically referred to as a quarter car model) can be developed. This model was (and still is) very popular in the automotive engineering community, especially before the widespread use of computer simulation, the reason being that the quarter car model, despite its simplicity, features the main variables of interest to suspension performance assessment: body acceleration, dynamic tyre force and suspension working space [SH86]. A merit of the quarter car is that it permits to evaluate more straightforwardly the effects of modifications in control parameters because higher-order dynamics and cross-coupling terms with the other suspension units are not taken into account. A good suspension design should produce improvement of both vehicle road holding and passenger comfort (or possibly improvement of one without degradation of the other), although inherent trade-offs are unavoidable in the design of a passive suspension system.

The quarter car is a 2 DOF system having two translational degrees of freedom. Another classical model can be obtained with only 2 DOF: the half vehicle model having a translational degree of freedom and a rotational degree of freedom to describe, respectively, bounce and pitch motions or, analogously, bounce and roll motions (in the former case the model is referred to as a bicycle model). Its natural extension is a 4 DOF model, which also includes tyre masses and elasticity. This model can be

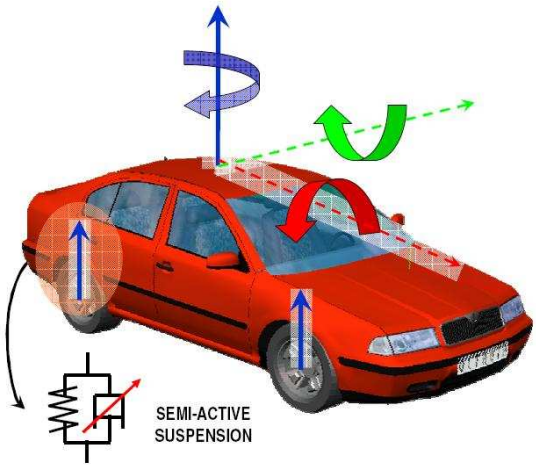

Figure 2.2 Vehicle Model (for vertical dynamics only).

employed to study the vehicle pitch (or roll) behaviour. However, the 4 DOF model cannot take into account the cross-couplings between the right- and left-hand side of the car (or front and rear in the case of roll motion). These interactions can be taken into account only by using a 7 DOF mode (sometimes referred to as a full car model) see Figure 2.2 , which allows one to represent bounce, roll and pitch motions. The models mentioned above are classical ride models. Higher order ride models can be developed including further degrees of freedom, e.g., accounting for seat and engine mounting elasticity. Driver and passengers can be modelled as well with springs, masses and damping elements. This is particularly important for accurate human comfort studies. Analogously to ride vehicle models, also handling models having different degrees of complexity can be developed. The equivalent handling model of the quarter car is a linear single track model which describes lateral and yaw dynamic responses to handling manoeuvres (ignoring the effect of sprung and unsprung masses).

Models including both ride and handling dynamics are necessary when there is a need to accurately investigate the interaction between ride and handling (during

a turning manoeuvre, for instance) and to study the limit of handling characteristics or elements such as anti-roll bars. Multi body techniques allow relatively easy development of complicated models with many degrees of freedom.

Analogously to cars, several heavy and trailed vehicles tractor and/or semi-trailer models [SH86] and [Won08] have been developed to examine their ride comfort, tractort/railer interactions, dynamic tyre forces and road damage. A survey can be found in [JSEG01]. These vehicle models usually include linear tyre models, linear or nonlinear suspension characteristics, tandem or single axles. Other truck ride models include suspended tractor cab and driver seat with linear or non-linear components. The models described and the simulation results presented in this thesis are based on the use of MATLAB and Simulink software.

2.2.2 Types of Suspensions Control System

Additional areas of confusion with terminology include the distinction amongst: passive, semi-active and active suspension systems.

- *passive systems* are classified as those that are only able to dissipate energy and that require no external energy sources to operate.
- *Fully active systems* are classified as those that supply energy to the systems, generally in the form of a force generating element in parallel to, or in place of, the passive suspension components.
- *Semi-Active systems* are classified as those that vary system parameters, but do not supply energy to the suspension system itself; these systems are only able to dissipate energy.

Semi-active systems are essentially variable dampers or springs. Semi-active systems do require external power, but far less than their fully active counterparts. To

see this, consider the power needed to vary the orifice size on a variable damper, to the power needed to move the suspension through its operating range. And for that we are decide to illustrate the feature of MR Controllable Damper.

2.3 MR Damper and Parameters Estimation

Most active suspension systems in production today are of semi-active type, so we are going to show the similarities of the Design of semi-active MR damper see also 5.4 .

2.3.1 Design of Magneto-rheological Damper

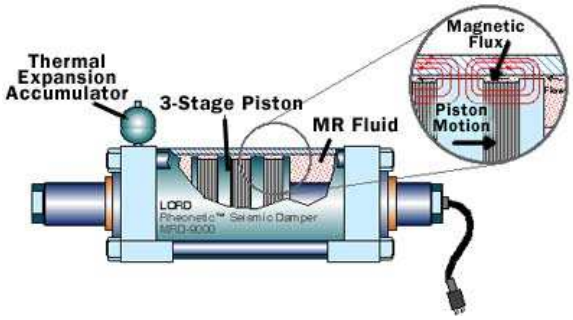

Figure 2.3 Magneto-rheological Dampers.

The prototype MR damper works in flow mode as shown in Figure 5.5. The damper is 218 mm long in its extended position, and has ± mm stroke. The main cylinder houses a piston, a magnetic circuit, an accumulator and MR fluid. MR 132 LD, which was obtained from Lord Corporation, is used in the damper [Htt]. The MR fluid valve is contained within the piston and consists of an annular flow channel with 1.5 mm gap. The magnetic field is applied radially across the gap, perpendicular to the direction of fluid flow. The total axial length of the flow channel is 6 mm which exposed to the applied magnetic field. Viscosity of MR fluid in the

valve will be increased by increasing the electric current through the electromagnet, thus resisting the MR fluid flow through the valve and increasing the damping force of the MR damper. The resistance of the electromagnet coil is 19 Ω.

To apply the MR damper in vibration control of vehicle suspension system, the property of the damper should be determined first and then a model must be developed that can accurately reproduce the behaviour of the MR damper. An experimental test rig is set up to determine the property of the MR damper and to obtain the dynamic data necessary for estimating the parameters of the model. In this test rig, the MR damper is fixed in a computer-controlled INSTRON Test Machine (Model 8874). The INSTRON Test Machine incorporates a load cell and a displacement sensor to measure the force produced by the MR damper and the displacement of the piston. Two types of excitations, sinusoidal and triangular, are used. The excitation frequencies are 1, 2 and 4 Hz and the amplitudes of excitation are 1, 2 and 4 mm, respectively. The applied electric current is from 0 to 1 A with increment of 0.25 A. The force and displacement responses of the damper are sampled simultaneously by the computer via an A/D converter. The excitation signal is also produced by the computer and sent out to the hydraulic actuator via a D/A converter. Velocity response can be obtained by differentiating the displacement. All experiments are carried out at the room temperature of 23 ℃.

2.3.2 Experimental Results

The responses of MR damper at 1 Hz excitation under five constant electric currents are shown in Figure 2.4. The effect of magnetic field on the damping force is clearly shown in these figures. With the increasing of the applied electric current, the damping force will increase remarkably, however when the applied electric current is more than 0.75 A, the increase of the damping force is no longer significant. This means

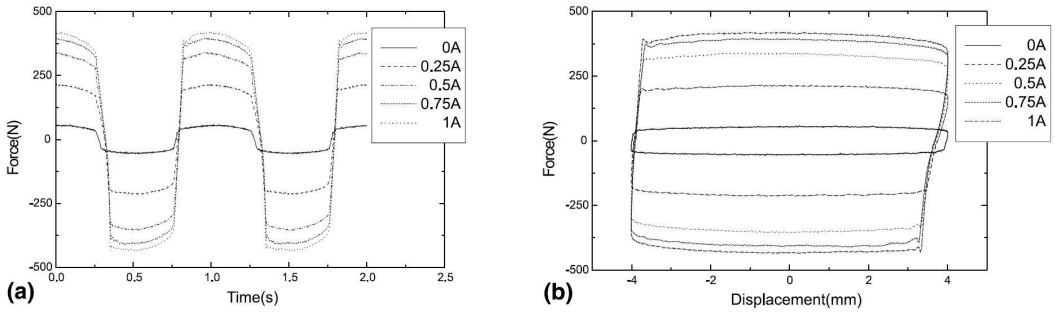

(a) Responses of force vs. time (b) Responses of force vs. displacement

Figure 2.4 Responses of force under different electric currents

that saturation of the MR effect occurs at 0.75 A. It is also noted that the force produced by the damper is not exactly centred at zero. This is due in part to the presence of an accumulator in the MR damper, which is filled with highly compressed air, and in part due to the existence of air in the cylinder since the damper cannot be fully filled with MR fluid. The maximum force of MR damper at 1 A is approximately equal to eight times of that without electric field. Similar results can be obtained from experiment at the other excitation frequencies and amplitudes. To obtain the relation of equivalent damping coefficient to velocity and electric current, experiments are done under the triangular excitation. The equivalent damping coefficient of the damper against velocity under various electric currents is shown in Figure 2.5. It is seen that at low velocity, equivalent damping coefficient will increase markedly. As the velocity increases, the equivalent damping coefficient under high electric current decreases rapidly whereas that without electric current decreases slowly. At high velocity, the effect of current on equivalent damping coefficient is also not so significant. This phenomenon means that the MR damper cannot be treated as a viscous damper under high electric current.

From the experiments, it is seen that the designed MR damper has very large changeable damping force range under magnetic field, although the saturated mag-

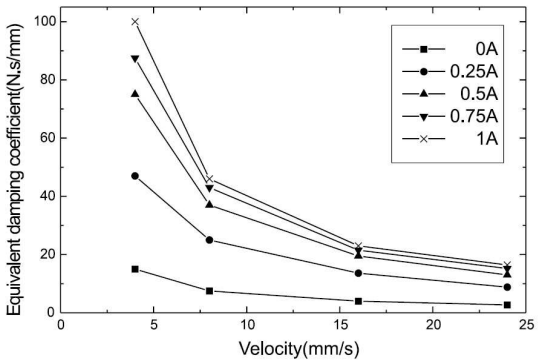

Figure 2.5 Equivalent damping coefficient vs. velocity

netic field is not so big. An improvement should be proposed to increase the saturated magnetic field and to avoid the side effect of the accumulator. Furthermore since the MR damper cannot be treated as a viscous damper under high electric current, a suitable model is necessary to be developed to describe the MR damper.

2.3.3 Applications of MR Technology in the Industry

Lord Magneto-Rheological (MR) technology enables new levels of performance in automotive primary suspension systems. In an MR suspension, controllable MR fluid replaces traditional hydraulic fluid in each shock absorber. As sensors monitor road and vehicle conditions, a controller modifies the damping characteristics up to one thousand times per second. This enables dramatic improvements in both ride comfort and handling.

Delphis MagneRide system incorporates LORD MR fluid to provide real-time optimization of suspension delphi.jpgdamping characteristics [**?**]. MagneRide is incredibly flexible it can be used to improve the driving characteristics of any vehicle, from high-end sports cars, to sedans and SUVs. First introduced in the 2002 model year, the system now appears on more than a dozen models from a wide variety

Figure 2.6 Delphis MagneRide (MR)system

of OEMs, including: *Acura MDX, Audi TT,Audi R8,Buick Lucerne, Cadillac DTS, Cadillac SLR, Cadillac SRX, Cadillac STS, Chevrolet Corvette, Ferrari 599GTB, Holden HSV Commodore.*

LORD MR Technology Advantages

Our controllable MR damping technology outperforms all existing passive and active suspension systems.

Unequaled shock and vibration control Lord MR systems offer unsurpassed effectiveness in precise, real-time control of mechanical systems, resulting in an unequaled ride experience. LORD MR-based suspensions are a no-compromise suspension solution that provides both firm cornering and superior isolation from road shocks and vibrations.

Fewer moving parts, less manufacturing complexity Delphis MagneRide shocks with LORD MR fluid have fewer moving parts than conventional controllable shocks 60 percent fewer parts than valve-based semi-active damper systems.

Low power consumption Lord MR suspension systems typically require very little power. In the MagneRide system, peak power is 20 watts at each of the system's four dampers.

Quieter operation Lord MR dampers are also quieter in operation than those based on conventional servo-valve technology.

Durability-tested and approved Our MR technology has surpassed all automotive durability testing for primary suspension shocks and is endorsed by two leading component manufacturers. The durability of this technology is further validated by more than five years of production and billions of incident-free road miles in Class 8 vehicle seat suspensions.

2.4 Vehicle Motion

Vehicle motion is described in a standard way as well. These motions and the relative axes are shown in Figure 2.7. The vertical motion of the sprung mass is referred to as heave, and is usually measured at the sprung mass center of mass. The rotational motion along an axis parallel to the vehicle axles is referred to as pitch. Nose-dive during vehicle braking is an example of the excitation of pitch motion. Roll is rotational motion about an axis that spans the length of the vehicle. One roll motion excitation source is cornering. Angular motion about an axis perpendicular to the ground is called yaw. Excessive yaw results in vehicle spin-out.

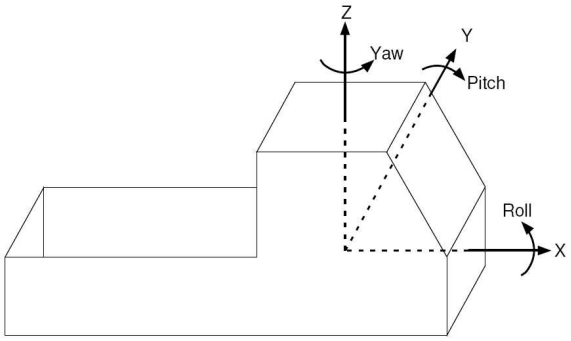

Figure 2.7 Orientation of Axes.

2.5 Tyre Modelling

Tyres are made of rubber, *i.e.*, a viscoelastic material and usually, in ride studies, the vertical tyre stiffness is approximated by a spring and some damping, either pure viscous or hysteretic damping, but often negligible. The tyre is represented as a spring plus a viscous damping term. This model, although quite crude, is acceptable for ride analysis. Handling, braking or traction studies require more sophisticated models which account for road-tyre adhesion along both longitudinal and lateral axes as well as rolling frictions.

The majority of studies utilise a point contact model since it is easy to use. Such a model has at least two defects. Firstly, the point follows the slightest vertical excursion of the road and hence generates high-frequency inputs which in practice would not occur as the tyre contact patch bridges or envelops such points.

For on-road applications, it is valid to regard the road profile as rigid compared to the flexible tyre. The main difficulty is locating the point of contact for each spring when a pseudo-random road profile is assumed. Such a model generates longitudinal forces but does not admit enveloping, although [Dav75] has extended the model to allow it. Torsional tyre distortion is usually not modelled.

2.6 Road Modelling

The representation of the road profile is vital for vehicle dynamic simulations because it is the main source of excitation. An accurate road model is as important as a good vehicle model. Sources of vehicle vibration include forces induced by road surface irregularities as well as aerodynamic forces and vibration that arise from the rotating mechanical parts of the vehicle tyres, engine and transmission [GSS+08]. However, the road surface elevation profile plays the major rule. Road roughness includes any type of surface irregularities from bump and potholes to small deviations. The reduction of forces transmitted to the road by moving vehicles is also an important issue responsible for road damage. Heavy-vehicle suspensions should be designed accounting also for this constraint.

Road inputs can be classified into three types:

- Deterministic road, periodic and almost-periodic inputs.
- Random-type inputs.
- Discrete events such as humps and potholes.

As far as deterministic inputs are concerned, a variety of periodical waveforms can be used, such as sine waves, square waves or triangular waves. To a first approximation the road profile can be assumed to be sinusoidal. Although not realistic, it is useful in a preliminary study because it readily permits a comparison of the performance of different suspension designs both in the time and in the frequency domain through permissibility charts, plotted at different frequencies.

A multi-harmonic input which is closer to an actual road profile can be generated. A possible choice which approximates fairly well a real road profile is a

so-called pseudo-random input [Duk00] which results from summing several non-commensurately related sine waves (i.e.. the ratio of all possible pairs of frequencies is not a rational number) of decreasing amplitude, so as to provide a discrete approximation of a continuous spectrum of a random input. The trend can be proved to be non-periodic, sometimes referred to as almost periodic in spite of being a sum of periodic waveforms [Duk00]. To achieve a pseudo-random profile effect it is advisable to select spatial frequencies of the form:

$$j\triangle\Omega + transcendentalterm \quad j = 1, ..., m. \tag{2.1}$$

where j is an integer, $\triangle\Omega$ is the separation between spatial frequencies and the added term could be $e/1000$ or $\pi/I000$ for example. The spatial frequency range is $(m - I)\triangle\Omega)$. The RMS amplitude at each centre frequency is obtained from the power spectral law and multiplication by $\triangle\Omega$.

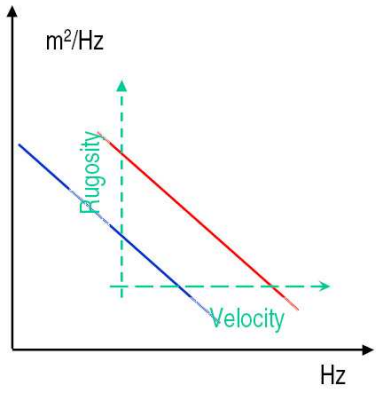

Figure 2.8 Spatial Road Profile (model input).

Another possible way to generate a realistic multi-harmonic input consists in making the ratio between frequencies constant and decreasing with amplitude, by using randomly generated phase angles between 0 and 360 degrees for each component. In this case, the resulting waveform is periodical. Simulation results presented subse-

quently are based on the latter approach.

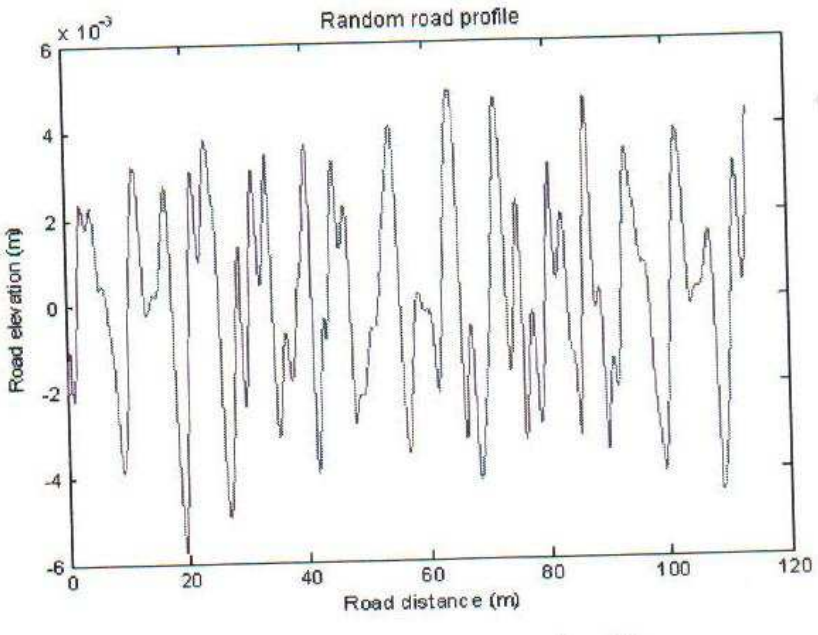

Figure 2.9 Pseudo-Random Road Profile [GSS+08] .

Figure 2.9 shows an example of road profile: 20 sine waves with random phases have been added together in order to create a pseudo-random profile. The amplitude of the profile is calculated to approximate a smooth highway by using the spatial frequency data suggested by the Society of Automotive Engineers (SAE).

However, these road profiles are deterministic functions and as a consequence could not represent a real random pavement. A stochastic model gives the more realistic representation of a road profile. The power spectral density (PSD) is the most common way to characterise the road roughness, a road could well be approximated [Won08] by an ergodic process with spectral density expressed by:

$$S(\Omega) = C\Omega^{-n} \tag{2.2}$$

where Ω is the spatial frequency, having units of $cycles/m$ (i.e., Ω is the inverse

of wavelength), C is a coefficient dependent on the road roughness, f the frequency in Hz and n is a rational exponent see Figure 2.8 . It follows that $\Omega = f/V$ where V is the forward speed of the car, so that:

$$S(f) = (\frac{C}{V^{-n}})f^{-n} \tag{2.3}$$

This approach involves an analysis in terms of power spectral densities. For a linear system the input and output spectral densities $Y_{in}(f)$ and $Y_{out}(f)$ are related through the transfer function of the system $G(f)$, from the equation:

$$Y_{out}(f) = |G(f)|^2 Y_{in}(f) \tag{2.4}$$

This property in the frequency domain only applies to linear systems and allows the output spectral density to be readily calculated if the vehicle transfer function and the input spectral density are known. For a non-linear system this property does not hold true.

2.7 Simple Car Model

Many metrics have been introduced for evaluating ride comfort including root mean square *(RMS)* vertical acceleration, *(RMS)* jerk (derivative of acceleration), frequency dependent or weighted accelerations, and rotational accelerations. Most active suspension researchers agree, however, that RMS acceleration is an adequate measure to quantify the improvements possible through active suspension control. Additional justification for using only RMS vertical acceleration was found by [Gil92].

About the choice of the type of model there are many different considerations. Many models only deal with vertical motions and cannot take into account the pitch, roll and yaw motions [LRG01]. Half-car pitch-plane models (bicycle models) are

often considered to perform good handling capabilities (steering control). However they do not include roll motions. Finally, some papers study complete vehicle model but the four suspension elements are assumed to be independent which is not the case in most vehicles. We will use quarter- and half-car models just for comparison between them, with and without consideration of the passengers dynamics in the simulation.

2.7.1 Quarter-Car Model

It is useful to introduce the vocabulary that will be used throughout the remainder of this thesis. These terms can be introduced in the context of the quarter-car model shown in Figure 2.10. The mass supported by the vehicle suspension is referred to as the sprung mass. All other vehicle mass, which includes all suspension components, vehicle axle assemblies, and vehicle tires and wheels is referred to as unsprung mass. A typical ratio of sprung to unsprung mass is 10:1 see [Gil92]. This ratio will be used for the unloaded cases throughout most of the work here.

The quarter-car has been for a long time been the most used model in suspension design. It is very simple as it can only represent the bounce motion of the chassis and wheel without taking into account pitch or roll vibration modes. However, it is very useful for a preliminary design: it is described by the following system of second-order.

A two-degree-of-freedom quarter-car model is depicted in Figure 2.10 In this model, the sprung and unsprung masses corresponding to the one corner of the vehicle are denoted, respectively, by m and m_t. The suspension system is represented by a linear spring of stiffness k and a linear damper with a damping rate c, whereas the tire is modelled by a linear spring of stiffness k_t and linear damper with a damping rate c_t, x is vertical displacement of the chassis), x_t is vertical displacement of the tyre.

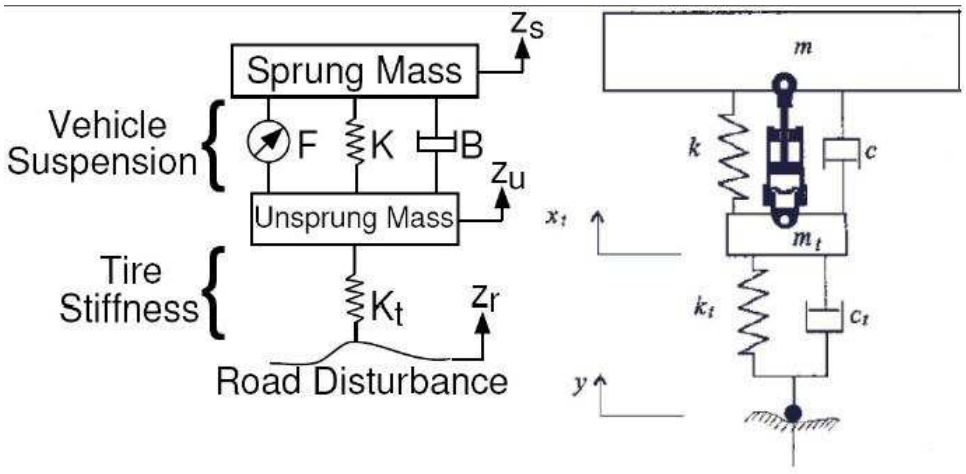

Figure 2.10 Quarter-car suspension model [KZ06] .

The excitation comes from the road irregularity y. The model is generally reputed to be sufficiently accurate for capturing the essential features related to discomfort, road holding, and working space [Gob01]. The linear equations of motions of the system model are:

$$\ddot{x} = -\frac{1}{m}(k)x + \frac{1}{m}kx_t + \frac{1}{m}c\dot{x}_t - \frac{1}{m}c\dot{x} + \frac{F}{m} \tag{2.5}$$

$$\ddot{x}_t = \frac{1}{m_t}(kx - (k+k_t)x_t + k_t y - F) + \frac{1}{m}(c\dot{x} - (c+c_t)\dot{x}_t + c_t\dot{y}) \tag{2.6}$$

The equations of motion of the suspension system can be written in compact form as:

$$\dot{z} = Az + Bu + Gw \tag{2.7}$$

where the state vector z, is given by:

$$z = [x\ x_t\ \dot{x}\ \dot{x}_t]^T \tag{2.8}$$

The vector w represents the road disturbance:

$$w = [y\ \dot{y}]^T \tag{2.9}$$

and the vector u represents the damper forces:

$$u = [F]^T \tag{2.10}$$

The matrices $A \in R^{4\times4}, B \in R^{4\times1}, andG \in R^{4\times2}$

Table 2.1 Quarter Car Suspension Parameters.

Notation	Description	Units	Values
m	Chassis mass	Kg	900
m_t	axle mass	Kg	90
k	main stiffness	Kg	18615
c	main damping	N s/m	1000
k_t	tire stiffness	N/m	500
c_t	tyre damping	N s/m	1100

2.7.2 Half Car Model

Figure 2.11 shows a half-car model, which has four degrees of freedom. The model consists of the chassis and two axles. It is assumed that the chassis has both bounce and pitch and the axles have independent bounce oscillations. The suspension and tyre are modelled using linear springs in parallel with viscous dampers [TE98]. Two MR dampers are used to provide controllable forces, and are located parallel to the suspension springs and shock absorbers. To derive the equations of motion for the half-car, the notation given in table 2.4 is adopted. The four degrees of freedom are:

x (vertical displacement of the chassis),θ (rotational displacement of the chassis), x_{t1} (vertical displacement of tyre 1), and x_{t2} (vertical displacement of tyre 2).

Summing up all forces acting on all masses and moments about the center of gravity of the chassis leads to the following equations:

$$\begin{aligned}
\ddot{x} &= -\frac{1}{m}(k_1+k_2)x - \frac{1}{m}(k_1b_1+k_2b_2)\theta + \frac{k_1}{m}x_{t1} + \frac{k_2}{m}x_{t2} \\
&\quad - \frac{1}{m}(c_1+c_2)\dot{x} - \frac{1}{m}(c_1b_1-c_2b_2)\dot{\theta} + \frac{F_{1+F_2}}{m} \\
\ddot{\theta} &= -\frac{1}{I_p}(k_1b_1+k_2b_2)x - \frac{1}{I_p}(k_1b_1^2+k_2b_2^2)\theta - \frac{k_1b_1}{I_p}x_{t1} \\
&\quad + \frac{k_2b_2}{I_p}x_{t2} - \frac{c_1b_1}{I_p}\dot{x}_{t1} + \frac{c_2b_2}{I_p}\dot{x}_{t2} - \frac{1}{I_p}(c_1b_1-c_2b_2)\dot{x} \\
&\quad - \frac{1}{I_p}(c_1b_1^2+c_2b_2^2)\dot{\theta} + \frac{1}{I_p}(F_1b_1+F_2b_2) \\
\ddot{x}_{t1} &= \frac{1}{m_{t1}}(k_1x + k_1b_1\theta - (k_1+k_{t1})x_{t1}y_1 - F_1) \\
&\quad + \frac{1}{m_{t1}}(c_1\dot{x} + c_1b_1\dot{\theta} - (c_1+c_{t1})\dot{x}_{t1} + c_{t1}\dot{y}_1) \\
\ddot{x}_{t2} &= \frac{1}{m_{t2}}(k_2x + k_1b_2\theta - (k_2+k_{t2})x_{t2}y_2 - F_2) \\
&\quad + \frac{1}{m_{t2}}(c_2\dot{x} + c_2b_2\dot{\theta} - (c_2+c_{t2})\dot{x}_{t2} + c_{t2}\dot{y}_2)
\end{aligned} \tag{2.11}$$

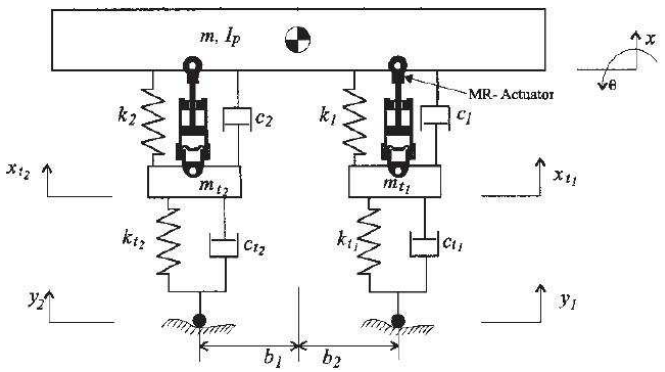

Figure 2.11 Half-car suspension model [KZ06].

The equations of motion of the suspension system can be written in compact form as:

$$\dot{z} = Az + Bu + Gw \tag{2.12}$$

where the state vector z, is given by:

$$z = [x\ \theta x_{t1}\ x_{t2}\ \dot{x}\ \dot{\theta}\ \dot{x}_{t1}\ \dot{x}_{t2}]^T \tag{2.13}$$

The vector w represents the road disturbance:

$$w = [y_1\ y_2\ \dot{y}_1\ \dot{y}_2]^T \tag{2.14}$$

and the vector u represents the damper forces:

$$u = [F_1\ F_2]^T \tag{2.15}$$

The matrices $A \in R^{8\times8}, B \in R^{8\times2}, andG \in R^{8\times4}$

2.8 Human Body Response

The apparent mass resonance frequency is in the range $5.4Hz$ to $4.2Hz$ as the magnitude of vibration increased from $0.25m/s$ $102.5m/s$. Various detailed models of the human body exist [GSS+08]. However, cushion and visceral natural frequencies are below $6Hz$. Moreover, because the amplitude of road profile fluctuations falls with decreasing wavelength, road inputs experienced by vehicle occupants are predominantly at low frequency. For realistic vehicle speeds higher frequency inputs are not important until wheel-hop is experienced at around $12Hz$ for cars and near 10 Hz for freight vehicles. When traversing rough ground drivers instinctively slow, reducing the frequency of input.

Table 2.2 Half Car Suspension Parameters.

Notation	Description	Units	Values
m	Chassis mass	Kg	1794
m_{t1}	front axle mass	Kg	87.15
m_{t2}	rear axle mass	Kg	140.04
I_p	Chassis inertia	Kg m^2	3443
k_1	front main stiffness	Kg	66824.0
k_2	rear main stiffness	Kg	18615.0
c_1	front main damping	N s/m	1190
c_2	rear main damping	N s/m	1000
k_{t1}	front tire stiffness	N/m	500
k_{t2}	rear tire stiffness	N/m	500
c_{t1}	front tyre damping	N s/m	1190
c_{t2}	rear tyre damping	N s/m	1000
b_1	distance	m	1271
b_2	distance	m	1713

2.8.1 Low-frequency Seated Human Model

The model adopted for the human body is one of those developed by [WG98]. This is shown in the upper part of Figure 2.12. The non-linear spring K_v models the stiffness effects with hysterical effects providing damping.

The motion of the visceral mass M_v is denoted by x, and that of the remainder M_c of the body by y. This second mass could be that of the skeleton. The authors also produced a two-degree-of-freedom model in order to model response at frequencies greater than about $8Hz$ [GSS$^+$08]. Vehicle simulations using this model indicated

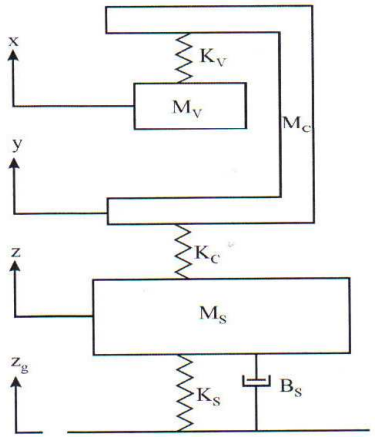

Figure 2.12 Vehicle and occupant model [GSS+08].

no significantly different response for realistic road inputs and vehicle speeds. Hence the single-degree-of freedom model is adopted here.

The seat is modelled as a mass M_s and a (non-linear) spring K_s. As indicated above the damping terms are deduced from a hysteric model. A seat control force F_c is considered. This would be provided by an actuator fixed to the vehicle floor beneath the seat.

The sprung mass M_s, on a spring and damper suspension, is modelled because it acts as a low-pass filter of road inputs. In the frequency range of interest, the unsprung mass is neglected as it is common with truck models. [in his experimental work using vertical inputs indicates a natural frequency of the human body in the range $4.2 - 5.4Hz$, depending on the amplitude of input [MG00].

2.8.2 Multy Frequency Input

Vehicle-occupant model for low-frequency vibrations is depicted in Figure 2.12. Ground input is indicated by z_g. The unsprung mass is not modelled as at the low frequencies is considered below $6Hz$. M_s represents the sprung mass of the vehi-

cle, restrained by a linear spring and viscous damper. The cushion is modelled as a complex spring K_c with loss factor β_c; M_c and M_v, represent the two masses of the Wei and Griffin 1 DOF model [Wei98], with K_v a non-linear spring with loss factor β_v.

The equations of motion for an input z_g of frequency ω are:

$$\begin{aligned}
\ddot{x} &= \omega_v^2 u(1-\epsilon_v u^2) + \omega_v^2 \beta_v \dot{u} \frac{(1+\epsilon_v \frac{\dot{u}^2}{\omega^2})}{\omega} \\
\ddot{y} &= -R\ddot{x} + (R+1)\omega_c^2 w(1-\epsilon_c w^2) + (R+1)\omega_c^2 \beta_c \dot{w} \frac{(1+\epsilon_v \frac{\dot{w}^2}{\omega^2})}{\omega} + \frac{F_c}{M_c} \\
\ddot{z} &= \omega_s^2(z_g - z) + 2\zeta\omega_s(\dot{g} - \dot{z}) - \frac{F_c}{M_c}
\end{aligned} \tag{2.16}$$

where $u = y - x$, $w = z - y$ and $R = \frac{M_v}{M_c}$; ω_v is the natural frequency of the linear visceral system. ω_c is the natural frequency of the total mass $M_v + M_c$ on the linear cushion. ω_s is the natural frequency of the sprung mass on its suspension. z_g is the road surface displacement as experienced by the vehicle [GSS+08].

The damping can be calculated by summing the contributions obtained from Individual frequency inputs [Wet97]. However, this procedure requires the amplitude of vibration at each frequency to be known, calling for a continuous FFT of the response. This would not appear practical and would certainly add expense to the system. The somewhat less elegant solution of selecting a typical ω is the strategy adopted here. The power: the spectral density for the road is defined over a range $[\Omega_1, \Omega_2]$ of the spatial frequency Ω (cycles/m), the frequency (Hz) experienced by a vehicle moving at speed V is $V\Omega$. The excitation has the form

$$\sum a_j \sin(2\pi\Omega_j V t + \varphi_j)$$

where Ω_j is a spatial frequency (cycles/m). V the vehicle speed and φ_j a random phase angle; $\dot{g}$ is the time derivative

$$\sum a_j 2\pi\Omega_j V \cos(2\pi\Omega_j V t + \varphi_j)$$

of the road surface displacement. This model can be used to obtain the frequency response of the system, be it passive or controlled.

2.9 Passenger Car Model

Two different others models will be used in this thesis: one is based on a Quarter Car Passenger Model and the other on the Half Car Passenger Model, but in this case we decided to take in consideration not just the model of vehicle but also the passengers inside the vehicle. The models are derived with values and dimensions obtained from a virtual prototype based on a real vehicle [KZ06].

2.9.1 Quarter Car Passenger Model

Quarter-car models with passengers consist of the wheel, unsprung mass, sprung mass, seats with passengers and suspension components (see Figure 2.13). Wheel is represented by the tire, which has the spring character. Wheel weight, axle weight and everything geometrically below the suspension are included in unsprung mass. Sprung mass represents body or in other words, chassis of the car. Suspensions consist of various parts. This model has been used extensively in the literature and captures many essential characteristics of a real suspension system. The equations of motion of the suspension system are:

$$\ddot{x} = -\frac{1}{m}(k+k_p)x + \frac{1}{m}k_p x_p + \frac{1}{m}kx_t + \frac{1}{m}c_p\dot{x}_p + \frac{1}{m}c\dot{x}_t - \frac{1}{m}(c+c_p)\dot{x} + \frac{F}{m} \quad (2.17)$$

$$\ddot{x}_t = \frac{1}{m_t}(kx - (k+k_t)x_t + k_t y - F) + \frac{1}{m}(c\dot{x} - (c+c_t)\dot{x}_t + c_t\dot{y}) \quad (2.18)$$

$$\ddot{x}_P = \frac{1}{m_P}(k_P x - k_P x_P) + \frac{1}{m_P}(c_P\dot{x} - c_P\dot{x}_P) \quad (2.19)$$

x is the position of the vehicle body center of gravity, x_t is the position of the wheel, x_p is the position of passenger and y is the displacements of the road see Figure 2.13. These differential equations can be rewritten in the compact form:

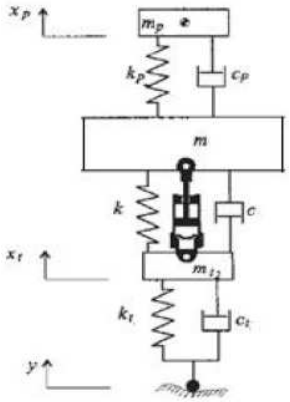

Figure 2.13 Quarter-car passenger suspension model [KZ06].

$$\dot{z} = Az + Bu + Gw \quad (2.20)$$

where the state vector z, is given by:

$$z = [x\ x_p\ x_t\ \dot{x}\ \dot{x}_p\dot{x}_t]^T \quad (2.21)$$

The vector w represents the road disturbance:

$$w = [y\ \dot{y}]^T \quad (2.22)$$

and the vector u represents the damper forces:

$$u = [F]^T \tag{2.23}$$

The matrices $A \in R^{6\times6}, B \in R^{6\times1}, andG \in R^{6\times2}$

Table 2.3 Quarter Car Passenger Suspension Parameters.

Notation	Description	Units	Values
m	Chassis mass	Kg	900
m_t	axle mass	Kg	90
m_p	Passenger mass	Kg	75
k	main stiffness	Kg	18615
c	main damping	N s/m	1000
k_t	tire stiffness	N/m	500
k_p	seat stiffness	N/m	14000
c_t	tyre damping	N s/m	1100
c_p	seat damping	N s/m	1000

2.9.2 Half Car Passenger Model

Figure 2.14 shows a half-car passenger model system, which has six degrees of freedom. The model consists of the chassis, two axles, and two passengers. It is assumed that the chassis has both bounce and pitch, the axles have independent bounce, and the passengers have only vertical oscillations. The suspension, tyre, and passenger seats are modelled by using linear springs in parallel with viscous dampers [Gil92]. Two dampers are used to provide controllable forces, and are located parallel to the suspension springs and shock absorbers. To derive the equations of motion for the

half-car. The six degrees of freedom are: x is the vertical displacement of the chassis,θ is the rotational displacement of the chassis, x_{p1} is vertical displacement of passenger 1, x_{p2} is vertical displacement of passenger 2, x_{t1} is the vertical displacement of tyre 1, and x_{t2} is the vertical displacement of tyre 2. y_1 and y_2 are the displacements of the road surface at the front wheel and rear wheel respectively, I_p is the moment of inertia at the vehicle body's center of gravity. Summing up all forces on all 5 masses and the moments about the centre of gravity of the chassis leads to the following equations:

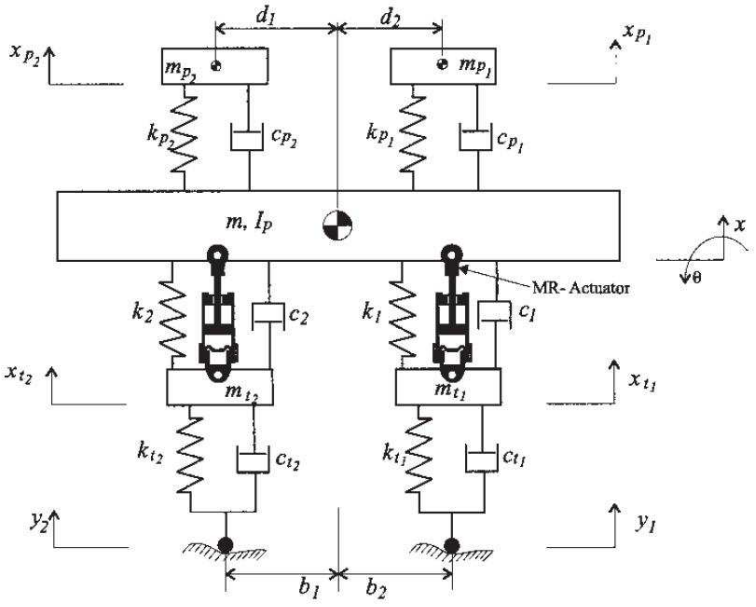

Figure 2.14 Half-car passenger suspension model [KZ06].

$$
\begin{aligned}
\ddot{x} &= -\frac{1}{m}(k_1+k_2+k_{p1}+k_{p2})x - \frac{1}{m}(k_1b_1+k_2b_2+k_{p1}d_1+k_{p2}d_2)\theta + \frac{k_{p1}}{m}x_{p1} + \frac{k_{p2}}{m}x_{p1} \\
&+ \frac{k_1}{m}x_{t1} + \frac{k_2}{m}x_{t2} + \frac{c_{p1}}{m}\dot{x}_{p1} + \frac{c_{p2}}{m}\dot{x}_{p2} + \frac{c_1}{m}\dot{x}_{t1} + \frac{c_2}{m}\dot{x}_{t2} - \frac{1}{m}(c_1+c_2+c_{p1}+c_{p2})\dot{x} \\
&- \frac{1}{m}(c_1b_1-c_2b_2+c_{p1}d_1-c_{p2}d_2)\dot{\theta} + \frac{F_1+F_2}{m} \\
\ddot{\theta} &= -\frac{1}{I_p}(k_1b_1-k_2b_2+k_{p1}d_1-k_{p2}d_2)x - \frac{1}{I_p}(k_1b_1^2+k_2b_2^2+k_{p1}d_1^2+k_{p2}d_2^2)\theta - \frac{k_{p1}d_1}{I_p}x_{p1} \\
&+ \frac{k_{p2}d_2}{I_p}x_{p2} - \frac{k_1b_1}{I_p}x_{t1} + \frac{k_2b_2}{I_p}x_{t2} - \frac{c_{p1}d_1}{I_p}\dot{x}_{p1} + \frac{c_{p2}d_2}{I_p}\dot{x}_{p2} - \frac{c_1b_1}{I_p}\dot{x}_{t1} + \frac{c_2b_2}{I_p}\dot{x}_{t2} \\
&- \frac{1}{I_p}(c_1b_1-c_2b_2+c_{p1}d_1-c_{p2}d_2)\dot{x} - \frac{1}{I_p}(c_1b_1^2+c_2b_2^2+c_{p1}d_1^2+c_{p2}d_2^2)\dot{\theta} + \frac{1}{I_p}(F_1b_1-F_2b_2) \\
\ddot{x}_{t1} &= \frac{1}{m_{t1}}(k_1x+k_1b_1\theta-(k_1+k_{t1})x_{t1}+k_{t1}y_1-F_1) + \frac{1}{m_{t1}}(c_1\dot{x}+c_1b_1\dot{\theta}-(c_1+c_{t1})\dot{x}_{t1}+c_{t1}\dot{y}_1) \\
\ddot{x}_{t2} &= \frac{1}{m_{t2}}(k_2x+k_1b_2\theta-(k_2+k_{t2})x_{t2}+k_{t2}y_2-F_2) + \frac{1}{m_{t2}}(c_2\dot{x}-c_2b_2\dot{\theta}-(c_2+c_{t2})\dot{x}_{t2}+c_{t2}\dot{y}_2) \\
\ddot{x}_{p1} &= \frac{1}{m_{p1}}(k_{p1}x+k_{p1}d_1\theta-(k_{p1}x_{p1}) + \frac{1}{m_{p1}}(c_{p1}\dot{x}+c_{p1}d_1\dot{\theta}-c_{p1}\dot{x}_{p1}) \\
\ddot{x}_{p2} &= \frac{1}{m_{p2}}(k_{p2}x+k_{p2}d_2\theta-(k_{p2}x_{p2}) + \frac{1}{m_{p2}}(c_{p2}\dot{x}-c_{p2}d_2\dot{\theta}-c_{p2}\dot{x}_{p2})
\end{aligned}
\tag{2.24}
$$

The equations of motion of the suspension system can be written in compact form as:

$$\dot{z} = Az + Bu + Gw \tag{2.25}$$

where the state vector z, is given by:

$$z = [x\ \theta x_{p1}\ x_{p2}\ x_{t1}\ x_{t2}\ \dot{x}\ \dot{\theta}\ \dot{x}_{p1}\ \dot{x}_{p2}\ \dot{x}_{t1}\ \dot{x}_{t2}]^T \tag{2.26}$$

The vector w represents the road disturbance:

$$w = [y_1\ y_2\ \dot{y}_1\ \dot{y}_2]^T \tag{2.27}$$

and the vector u represents the damper forces:

$$u = [F_1 \ F_2]^T \tag{2.28}$$

The matrices $A \in R^{12\times12}, B \in R^{12\times2}, andG \in R^{12\times4}$

Table 2.4 Half Car Suspension Parameters.

Notation	Description	Units	Values
m	Chassis mass	Kg	1794
m_{t1}	front axle mass	Kg	87.15
m_{t2}	rear axle mass	Kg	140.04
m_{p1}	rear Passenger mass	Kg	75
m_{p2}	rear Passenger mass	Kg	75
I_p	Chassis inertia	Kg m^2	3443
k_1	front main stiffness	Kg	66824.0
k_2	rear main stiffness	Kg	18615.0
c_1	front main damping	N s/m	1190
c_2	rear main damping	N s/m	1000
k_{t1}	front tire stiffness	N/m	500
k_{t2}	rear tire stiffness	N/m	500
k_{p1}	front seat stiffness	N/m	1190
k_{p2}	front seat stiffness	N/m	1000
c_{t1}	front tyre damping	N s/m	1190
c_{t2}	rear tyre damping	N s/m	1000
b_1	distance	m	1271
b_2	distance	m	1713
d_1	distance	m	0.481
d_2	distance	m	1.313

Chapter 3

Controller Design

During the last two decades, various types of structural active control strategies have been applied to the control of suspension structures. Depending on the available information for each controlled structure, viz. the mathematical model associated, the types of measurements, actuators and disturbances, each control solution can be suitable only for one specific type of structure and not for all kinds. In this dissertation, before starting with the study of our H-infinity optimal control algorithm, a particular instance of a mixed sensitivity control problem, we describe some others kind of control algorithms and discuss their industrial applications.

3.1 Control Algorithm

3.1.1 Optimal Control

The general optimal control problem may be stated as follows: given a system subjected to external inputs, find the control which minimizes a certain measure of the performance of the system. Optimal control algorithms are based on the minimization of a performance index that depends on the system variables, while maintain a

desired system state and minimize the control effort. According to classical performance criterion, the active control force u is found by minimizing the performance index subject to a second order system. The performance index can include a measure of operating error, a measure of control or any other variable which is important for the user of the control system. There are two control design objectives: Regulation problems, which consists of stabilizing the system around some equilibrium state so that its states and/or outputs remain small around it, and Tracking or Servo problems where the control is optimized for a certain prescribed output of the system to follow a desired trajectories while all states remain bounded. The main optimal control techniques derived in the literature are: the Linear Quadratic Regulator (LQR), Linear Quadratic Gaussian (LQG), Clipped Optimal Control and Bang-Bang Control.

LQR Control Algorithm

This technique is characterized by requiring that all state variables be available (measurable) for feedback. This control algorithm is the classical one used for active and semi-active control of structures. However, it is not always possible to use it for structural control due to the limitations on the number of sensors that could be installed in the large structures or for the presence of non-linearities in the structure or in the actuators.

Consider the LTI system

$$\begin{aligned} \dot{x} &= Ax + B_u u, \qquad x(0) = x_{0,} \\ z &= C_z x + D_{zu} u. \end{aligned} \tag{3.1}$$

where $D_{zu}^T D_{zu} \succ \Theta$ and the cost function

$$\begin{aligned} J &= \int_0^\infty z(t)^T z(t)\, dt, \\ &= \int_0^\infty x(t)^T \underbrace{C_z^T C_z}_{Q} x + 2x(t)^T \underbrace{C_z^T D_{zu}}_{S} u(t) + u(t)_T \underbrace{D_{zu}^T D_{zu}}_{R} u(t)\, dt \end{aligned} \tag{3.2}$$

The control that minimizes the cost function J over all possible controllers (including nonlinear controllers) is the state feedback law $u = Kx$ where:

$$K = -(D_{zu}^T D_{zu})^{-1}(B_u^T P + D_{zu}^T C_z)$$

and P is the stabilizing solution to the Riccati equation

$$A^T P + PA - (PB_u + C_z^T D_{zu})(D_{zu}^T D_{zu})^{-1}(B_u^T P + D_{zu}^T C_z) + C_z^T C_Z = \Theta$$

The optimal control achieves the optimal performance

$$J^* = \int_0^\infty z^*(t)^T z^*(t)\, dt \; = x_0^T P x_0.$$

A variation of LQR control is the Instantaneous Optimal Control, which uses a performance index as control objective similar to LQR control algorithm, but this does not need to solve the Riccati equation.

LQG Control Algorithm

In control, the Linear-Quadratic-Gaussian (LQG) control problem is probably the most fundamental optimal control problem. It concerns uncertain linear systems disturbed by additive white Gaussian noise, incomplete state information (i.e. not all the state variables are measured and available for feedback) also disturbed by additive white Gaussian noise and quadratic costs. Moreover, the solution is unique and constitutes a linear dynamic feedback control law that is easily computed and implemented. Finally, the LQG controller is also fundamental to the optimal perturbation control of non-linear systems [Ath03].

The LQG controller is simply the combination of a Kalman filter i.e. a Linear-Quadratic Estimator (LQE) with a Linear-Quadratic Regulator (LQR). The separation principle guarantees that these can be designed and computed independently. LQG control applies usually to linear time-invariant systems.

Finally, a word of caution. LQG optimality does not automatically ensure good robustness properties [GL]. The robust stability of the closed loop system must be checked separately after the LQG controller has been designed.

Now let's take some mathematical description of the problem and solution in the discrete-time only.

Since the discrete-time LQG control problem is similar to the one in continuous-time the description below focuses on the mathematical equations.

Discrete-time linear system equations:

$$\begin{aligned} x_{i+1} &= A_i x_i + B_i u_i + v_i \\ y_i &= C_i x_i + w_i \end{aligned} \tag{3.3}$$

Here i represents the discrete time index and v_i, w_i represent discrete-time Gaussian white noise processes with covariance matrices V_i, W_i respectively. The quadratic cost function to be minimized:

$$J = E(x_N^{'} F x_N + \sum_{i=0}^{N} -1 x_i^{'} Q_i x_i + u_i^{'} R_i u_i) \tag{3.4}$$

where $F \geq 0,\ Q_i \geq 0,\ R_i \geq 0$ The discrete-time LQG controller:

$$\begin{aligned} \hat{x}_{i+1} &= A_i \hat{x}_i + B_i u_i + K_i(y_i - C_i x_i), \ \ \hat{x}_0 = E(x_o) \\ u_i &= -L_i \hat{x}_i \end{aligned} \tag{3.5}$$

The Kalman gain equals,

$$K_i = A_i P_i C_i^{'} (C_i P_i C_i^{'} + W_i)^{-1}$$

where P_i is determined by the following matrix Riccati difference equation that runs forward in time,

$$P_{i+1} = A_i(P_i - P_i C_i^{'}(C_i P_i C_i^{'} + W_i)^{-1} C_i P_i)A_i^{'} + V_i, \quad P_0 = E(x_0 x_0^{'})$$

The feedback gain matrix equals,

$$L_i = (B_i^{'} S_{i+1} B_i + R_i)^{-1} B_i^{'} S_{i+1} A_i$$

where S_i is determined by the following matrix Riccati difference equation that runs backward in time,

$$S_i = A_i^{'}(S_{i+1} - S_{i+1} B_i (B_i^{'} S_{i+1} B_i + R_i)^{-1} B_i^{'} S_{i+1}) A_i + Q_i, \;\; S_N = F$$

if all matrices in the problem formulation are time-invariant and if the horizon N tends to infinity the discrete-time LQG controller becomes time-invariant. In that case, the matrix Riccati difference equations may be replaced by their associated discrete-time algebraic Riccati equations. These determine the time-invarant linear-quadratic estimator and the time-invariant linear-quadratic regulator in discrete-time. To keep the costs finite instead of J one has to consider J/N in this case.

Several applications of this theory have been made in civil engineering structures, both for active and semi-active control [YF00].

3.1.2 Predictive Control

The methodology of predictive control was introduced in 1974 by J.M Martin S. This principle can be defined as: Based on a model of the process, predictive control is the one that makes the predicted process dynamic output equal to a desired dynamic output conveniently predefined. The predictive control strategy may be generalized

and implemented through a predictive model and a driver block. The predictive control generates, from the previous input and output process variables, the control signal that makes the predicted process output equal to the desired output. In fact, predictive control results in a simple computational scheme with parameters, having clear physical meaning and handling of time delays related to the actuators in the control system.

Model Based Predictive Control

The performance of this technique depends significantly on the prediction made by the model. The basic strategy of predictive control implies the direct application of the control action in a single-step prediction. Thus the predictive control must be formulated in discrete time. At each sampling instant k, the desired output for the next instant $k+1$ is calculated, which is denoted by $y_d(k+1|k)$. The basic predictive control strategy can be summarized by the condition $\hat{y}(k+1|k) = y_d(k+1|k)$, whit $\hat{y}(k+1|k)$ the output predicted at instant k for the next instant $k+1$ and the control $u(k)$ to be applied at instant k must ensure the above condition. An essential feature of the model based predictive control is that the prediction for instant $k+1$, necessary to establish the control action $u(k+1)$, is made based on the information of the outputs $y(\cdot)$ and the inputs $u(\cdot)$ known at the instant k and at preceding instants. However, such prediction may differ from the real output, which will be measured at instant $k+1$, thus the real measurement at $k+1$ is used as the initial condition instead of the output that was predicted for this instant, which is essential for the effectiveness of the predictive control.

Adaptive Predictive Control

An adaptive predictive control system, consists in the combination of a predictive control system and an adaptive system. In an adaptive system, the predictive model gives an estimation of the process output at instant $k+1$ using the model parameters estimated at the instant k and the control signals and the process outputs already applied or measured at previous instants. The predictive model calculates the control action $u(k)$ in order to make the predicted output at instant $k+d$ equal to the driving desired output at the same instant. After a certain time required for adaptation, the process output should follow a driving desired trajectory (DDT) with a tracking error that is always bounded in the real case or is zero at the limit in the ideal case and the (DDT) should be physically realizable and bounded.

3.1.3 Robust Control

The principal objective of the robust control theory is to develop feedback control laws that are robust against plant model uncertainties and changes in dynamic conditions.

A system is robustly stable when the closed-loop is stable for any chosen plant within the specified uncertainty set and a system has robust performance if the closed-loop system satisfies performance specifications for any plant model within the specified uncertainty description. The need of using robust control in structural and suspensions control arises because the structural models contain appreciable uncertainty. This uncertainty may be expressed as bounds on the variation in frequency response or parametric variations of the plant. The mostly used robust control approaches in control of structures are the H_∞ control, the Lyapunov based control and the Sliding Mode Control.

Control Based on Lyapunov Stability Theory

Control based on Lyapunov stability theory consists of selecting a positive definite function denominated Lyapunov function. According to Lyapunov stability theory, if the rate of change of the Lyapunov function is negative semi-definite along the system trajectories, the closed-loop system is asymptotically stable (in the sense of Lyapunov). The objective of the control law is to select control inputs, which make the derivative of the Lyapunov function as negative as possible. The importance of this function is that it may contain the any variable that interests to be minimized (i.e. system states, control law error, control force, etc). In [RL98], a control input function is assumed to be continuous in state variables and linear in control action, but additionally admissible uncertainty is considered. Then, as a practical condition of stability, the ultimate boundedness of the system is demonstrated.

Basic Definition

Consider a dynamical system which satisfies:

$$\dot{x} = f(x,t) \qquad x(t_0) = x_0 \quad |; |x \in \mathrm{R}^n \tag{3.6}$$

We will assume that $f(x,t)$ satisfies the standard conditions for the existence and uniqueness of the solution. Such conditions are, for instance, that $f(x,t)$ is Lipschitz continuous with respect to x, uniformly in t, and piecewise continuous in t. A point $x^* \in \mathrm{R}^n$ is an equilibrium point of equation 3.6 if $f(x^*,t) = 0$. Intuitively and somewhat crudely speaking, we say an equilibrium point is locally stable if all solutions which start near x^* (meaning that the initial conditions are in a neighbourhood of x^*) remain near x^* for all time. The equilibrium point x^* is said to be locally asymptotically stable if x^* is locally stable and, furthermore,

all solutions starting near x^* tend towards x^* as $t \to \infty$. We say somewhat crude because the time-varying nature of equation 3.6 introduces all kinds of additional subtleties. Nonetheless, it is intuitive that a pendulum has a locally stable equilibrium point when the pendulum is hanging straight down and an unstable equilibrium point when it is pointing straight up. If the pendulum is damped, the stable equilibrium point is locally asymptotically stable.

By shifting the origin of the system, we may assume that the equilibrium point of interest occurs at $x_* = 0$. If multiple equilibrium points exist, we will need to study the stability of each by appropriately shifting the origin.

Definition of Stability in the sense of Lyapunov

The equilibrium point $x_* = 0$ of equation 3.6 is stable (in the sense of Lyapunov) at $t = t_0$ if for any $\epsilon > 0$ there exists a $\delta(t_0, \epsilon) > 0$ such that:

$$\|x(t_0)\| < \delta \Longrightarrow \|x(t)\| < \epsilon, \quad \forall t \geq t_0. \tag{3.7}$$

Lyapunov stability is a very mild requirement on equilibrium points. In particular, it does not require that trajectories starting close to the origin tend to the origin asymptotically. Also, stability is defined at a time instant t_0. Uniform stability is a concept which guarantees that the equilibrium point is not losing stability. We insist that for a uniformly stable equilibrium point x^*, δ in this Definition not be a function of t_0, so that equation 3.7 may hold for all t_0.

H_∞ Control

The H_∞ optimal control algorithm is the main algorithm for our control experiments in this dissertation. H_∞ control is a control design method where the H_∞ (induced) norm of the transfer function from the excitation u to controlled output y is designed

to be lower than a prescribed small value. The goal is to find a constant state-feedback matrix F to stabilize a plant P and to satisfy a given ∞ norm bound $||F1(P,F)||_\infty < \gamma$ on the closed-loop response. Because H_∞ control algorithm designs the controller in frequency domain, the frequency shape function can be used easily. It makes the control of specified frequency range possible and the spillover can be avoided. It is suitable for systems subject to unmodelled dynamics or unknown disturbances. In the next section we will provide more details about H_∞ optimal control theory.

3.2 H_∞ Theory

This thesis deals with the application of H_∞ optimal control for the design of an active suspension system. The involved vehicle is represented by both Quarter-car and half-car model, with and without the presence of passengers inside the car. A multi-variable H_∞ control is developed to satisfy the performance and comfort objectives. There is a wide range of optimal and robust controllers derived for a quarter car model and half Car Model. The classical approaches are based on H_∞ norm minimization. Essentially, it is an optimization method that takes into consideration a strong mathematical definition of the restrictions on the expected behaviour of the closed loop system and imposes strict stability conditions on it. Any advanced control methodology consists of finding a controller $K(s)$ for a plant model $G(s)$ such that the closed-loop system has good performances and robustness properties. The main advantage of the H_∞ control theory is that both the level of plant uncertainty and the gain from disturbance inputs to controlled outputs can be specified in the frequency domain. The H_∞ theory is appropriate for $MIMO$ systems. Let us first recall the H_∞ control problem. Next, we use in this chapter the mixed sensibility problem that

is presented as a particular case of the our H_∞ control problem.

3.2.1 Statement of H_∞ Control

In this section, a state space solution to the H_∞ control problem in the 2 input and 2 output block formulation will be presented. This solution was derived by Doyle et at. in 1988. The structure of this H_∞ solution will be compared to the well-known LQG structure, where it will be apparent that the two structures have several similarities [CAS01].

Hence, a solution will be given to the problem:

$$K(s) = \underset{K(s) \in k_S}{arg} \|F_l(N(s), K(s))\|_\infty \tag{3.8}$$

The problem of finding a solution to 3.8 was probably the most important research area within control theory during the 1980s. Initially, only algorithms that provided H_∞ optimal controllers of a very high order (see e.g. [Fra87]) were known, or algorithms that were only feasible for SISO systems (see e.g. [**?**]). However, Doyle, Clover, Khargonekar, and Francis announced a state space solution, involving only two algebraic Riccati equations, and yielding a compensator of the same order as the augmented system $N(s)$, just as for the well-known LQG solution. This was a major break-through for H_∞ theory. It is now evident that the LQG and the H_∞ control problems and their solutions were related in many ways. Both compensators have a state estimation-state feedback structure, and two algebraic Riccati equations provide the state feedback matrix K_c and the observer gain matrix K_f.

Given a 2 by 2 block matrix $N(s)$, see Figure 3.1, and a desired upper bound γ for the H_∞ norm $||F_l(N(s), K(s))||_\infty$, the H_∞ solution returns a compensator parametrization, often referred to as the DKGF parameterization:

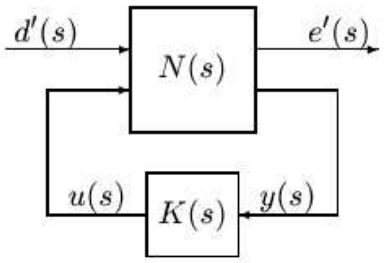

Figure 3.1 The 2 input and 2 output block problem [CAS01]

$$K(s) = F_l(J(s), Q(s)) \tag{3.9}$$

of all stabilizing compensators for which $||F_l(N(s), K(s))||_\infty < \gamma$, see Figure 3.2. Any stable transfer matrix $Q(s)$ for which $||Q(s)||_{H_\infty} < \gamma$ will stabilize the closed Loop system and make $||F_l(N(s), K(s))||_\infty < \gamma$. Any $Q(s)$ that, on the contrary, is unstable or has H_∞ norm larger than γ would either make the closed loop system unstable or imply that $||F_l(N(s), K(s))||_\infty \geq \gamma$.

The H_∞ solution is given by Definition 4.1 and by Theorem 4.1 [CAS01].

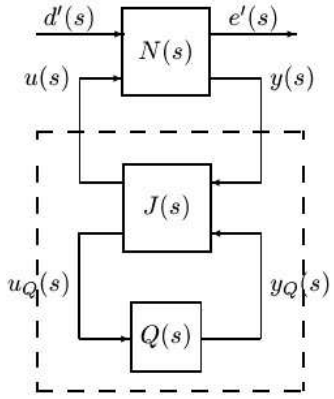

Figure 3.2 The DKGF parameterization of all stabilizing compensator [CAS01]

Definition 4.1 (Ricati Solution)

Assume that the algebraic Riccati equation

$$A^T X + XA - XRX + Q = O \tag{3.10}$$

has a unique stabilizing solution X, i.e. a solution for which the eigenvalues of$4RX$are all negative. This solution will be denoted by $X = Ric(H)$ where H is the associated Hamiltonian matrix

$$H = \begin{bmatrix} A & -R \\ -Q & -A^T \end{bmatrix} \tag{3.11}$$

Theorem 4.1 (The H_∞ Suboptimal Control Problem)

This formulation of the solution has been taken from [Dai90]. Let $N(s)$ be given by its slate space realization $A.B, C, D$ and introduce the notation:

$$N(s) = \left[\begin{array}{c|cc} A & B_1 & B_2 \\ \hline C_1 & D_{11} & D_{12} \\ C_2 & D_{21} & D_{22} \end{array}\right] \tag{3.12}$$

where B, C and D are partitioned consistently with d, e, u, and y. Now, make the following assumptions:

1. (A,B1) and (A,B2) are stabilizable (controllable).

2. (C1,A) and (C2,A) are detectable (observable).

3. $D_{12}^T D_{12} = I$and $D_{21} D_{21}^T = I$.

4. $D_{11} D_{22} = 0$.

where

$$\tilde{D_{12}} = I - D_{12} D_{12}^T, \qquad \tilde{D_{21}} = I - D_{21}^T D_{21} \tag{3.13}$$

and solve the two Riccati equations

$$X_\infty = Ric \begin{bmatrix} A - B_2 D_{12}^T C_1 & \gamma^{-2} B_1 B_1^T - B_2 B_2^T \\ -C_1^T \tilde{D_{12}}^T \tilde{D_{12}} C_1 & -(A - B_2 D_{12}^T C_1)^T \end{bmatrix} \tag{3.14}$$

$$X_\infty = Ric \begin{bmatrix} (A - B_1 D_{21}^T C_2)^T & \gamma^{-2} C_1^T C_1 - C_2^T C_2 \\ -B_1 \tilde{D_{21}} \tilde{D_{21}^T} B_1^T & -(A - B_1 D_{21}^T C_2) \end{bmatrix} \tag{3.15}$$

From the state feedback matrix K_c, the observer gain matrix K_f, and the matrix Z_∞ like:

$$K_c = (D_{12}^T C_1 + B_2^T X_\infty) K_f = (B_1 D_{21}^T + Y_\infty C_2^T) Z_\infty = (I - \gamma^{-2} Y_\infty X_\infty)^{-1} \tag{3.16}$$

if $X_\infty \geq 0$ and $Y_\infty \geq 0$ exist, and if spectral radius $\rho(X_\infty T_\infty) < \gamma^2$ then the DGKF parameterization is given by:

$$J(s) = \left[\begin{array}{c|cc} A_\infty & Z_\infty K_f Z_\infty (B_2 + \gamma^{-2} Y_\infty C_1^T D12) & \\ \hline -K_c & 0 & I \\ -(C_2 + \gamma^{-2} D_{21} B_1^T X_\infty) & I & 0 \end{array}\right] \tag{3.17}$$

where A_∞ is given by:

$$A_\infty = A - B_2 K_c + \gamma^{-2} B_1 B_1^T X_\infty - Z_\infty K_f (C_2 + \gamma^{-2} D_{21} B_1^T X_\infty) \tag{3.18}$$

Stabilizing compensators $K(s)$ satisfying $||F_l(N(s), K(s))||_\infty < \gamma$ can the be constructed by the combination of $J(s)$ with any stable $Q(s)$ for which $||Q(s)||_{H_\infty} < \gamma$:

$$K(s) = F_l(J(s), Q(s)) = J_{11}(s) + J_{12}(s) Q(s) (I - J_{22} Q(s))^{-1} J_{21}(s) \tag{3.19}$$

Then the H_∞ norm of the closed loop system $F_l(N(s), F_l(J(s), Q(s)))$ satisfies:

$$\|F_l(N(s), F_l(J(s), Q(s)))\|_\infty < \gamma \tag{3.20}$$

The compensator $J_{11}(s)$ obtained for $Q(s) = 0$ is called the H_∞ compensator.

Example of (CT-LTI) Systems

As an example of a continuous time, linear time-invariant (CT-LTI) system we consider:

$$\begin{aligned} \dot{x} &= Ax + B_w u + B_u u, \qquad x(0) = \Theta, \\ z &= C_z x + D_{zw} w + D_{zu} u. \end{aligned} \tag{3.21}$$

The Controller (state-feedback controller) is:

$$u = Kx$$

their Closed Loop System will be

$$\begin{aligned} \dot{x} &= (\underbrace{A + B_u K}_{A_{cl}})x + \underbrace{B_w}_{B_{cl}} w, |; \quad x_0 = \Theta \\ z &= \underbrace{(C_z + D_{zu} K)}_{C_{cl}} x + \underbrace{D_{zw}}_{D_{cl}} w. \end{aligned} \tag{3.22}$$

Now let's take the analysis conditions of $H\infty$ norm $\exists K \in \mathrm{R}^{mxn}$ such that

$$\|H_{cl}(K, s)\|_\infty < \mu$$

if, and only if, $\exists K \in \mathrm{R}^{mxn} and P \in \mathbb{S}^n$ such that (BRL)

$$P \succ \Theta, \quad \begin{bmatrix} A_{cl}^T P + P A_{cl} & P B_{cl} & C_{cl}^T \\ B_{cl}^T & -\mu I & D_{cl}^T \\ C_{cl} & D_{cl} & -\mu I \end{bmatrix} \prec \Theta$$

Method of congruence and change of variables

Apply the congruence transformation on the BRL

$$\begin{bmatrix} P^{-1} & \Theta & \Theta \\ \Theta & I & \Theta \\ \Theta & \Theta & I \end{bmatrix} \begin{bmatrix} A_{cl}^T P + P A_{cl} & P B_{cl} & C_{cl}^T \\ B_{cl}^T & -\mu I & D_{cl}^T \\ C_{cl} & D_{cl} & -\mu I \end{bmatrix} \begin{bmatrix} P^{-1} & \Theta & \Theta \\ \Theta & I & \Theta \\ \Theta & \Theta & I \end{bmatrix} \prec \Theta,$$

The matrices $B_{cl} = B_w$ and $D_{cl} = D_{zw}$ are constant matrices and the products

$$A_{cl}P^{-1} = AP^{-1} + B_u K P^{-1}, \quad C_{cl}P^{-1} = C_z P^{-1} + D_{zu} K P^{-1},$$

can be transformed into LMI using the change-of-variables $X := P^{-1},\ L := KX$.

Now we return at our (CT-LTI) system 3.21 that is stabilizable by the state feedback control $u = Kx$ such that

$$\|H_{cl}(K, s)\|_\infty < \mu$$

if, and only if, , $\exists X \in \mathrm{S}^n and L \in \mathbb{R}^{mxn}$ such that

$$X \succ \Theta, \begin{bmatrix} AX + XA^T + B_u L + L^T B_u^T & B_w & XC^T + L^T D_{zu}^T \\ B_w^T & -\mu I & D_{zw}^T \\ C_z X + D_{zu} L & D_{zw} & -\mu I \end{bmatrix} \prec \Theta.$$

If so, a stabilizing control gain is $K = LX^{-1}$ *Remarks*

- Optimal $H\infty$ control: minimize μ.
- This result can be used to provide stabilizability analysis of uncertain systems with norm bounded uncertainty.

3.2.2 Specifications with Mixed Sensitivity Functions

In this part of the thesis, the mixed sensitivity problem, which is a particular case of the H_∞ control problem, for multivariable systems [CAS01], the output sensitivity

functions introduced above can be defined based on the following feedback system presented on Figure 3.3 gives the structure of a process $G(s)$ and its controller $K(s)$, where w is a disturbance signal, Z_T are the outputs, Z_s are the outputs plus disturbance, and Z_M is the control signal. Then, the following relation holds:

$$\begin{pmatrix} Z_s \\ Z_T \\ Z_M \end{pmatrix} = \begin{pmatrix} S_0(s) \\ T_0(s) \\ M_0(s) \end{pmatrix} w \tag{3.23}$$

where:

- $S_0 = (I - GK)^{-1}$ (sensitivity)
- $M = K(I - GK)^{-1}$ (control sensitivity)
- $T_0 = GK(I - GK)^{-1}$ (complementary sensitivity)

In the sequel, it will be discussed how a feedback system can be designed based on specifications for the sensitivity. The approach is based on the following interpretation of the sensitivities:

Making the *sensitivity* $S_0(s)$ small implies:

- Good disturbance attenuation
- Good command following (bandwidth)

Making the *control sensitivity* $M(s)$ small implies:

- robustness additive uncertainties
- Moderate compensator gains
- Bonded impact of measurement noise

Making the *complementary sensitivity* $T_0(s)$ small implies:

- robustness additive uncertainties
- Bonded impact of measurement noise
- Moderate compensator gains

A fundamental trade-off, which must be reflected in any compensator design, manifested as the *complementary principal* is based on the following important observation:

$$S_0(s) - T_0(s) = I \tag{3.24}$$

this identity shows the existence of a intrinsic trade-off between performance and robustness, since S_0 and T_0 cannot be made small simultaneously.

Hence, any sensible synthesis method (H_∞ or others) must have the possibility to consider the pair (S_0,T_0) (or alternatively, the pair(S_0, M) with the perspective of deciding at each frequency ω whether $S_0(j\omega)$ or $T_0(j\omega)$ (alternatively: $S_0(j\omega)$ or $M(j\omega)$) should made small.

Such compensator design algorithms are collectively called *mixed sensitivity* methods

Application case with Mixed sensitivity problem

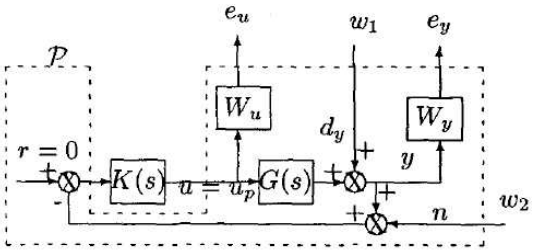

Figure 3.3 Mixed sensitivity problem as part of H_∞ control problem

u_p is the controlled input, y the output, r the reference, n a noise input due to the measurement and d_y the controlled output disturbance.

Let us defined the usual sensitivity functions:

$$\begin{cases} S_y = (I + GK)^{-1} \\ T_y = (I + GK)^{-1}GK \end{cases} \quad \begin{cases} S_y = (I + GK)^{-1} \\ T_y = (I + GK)^{-1}GK \end{cases} \tag{3.25}$$

with this notation we have:

$$\begin{aligned} y &= S_y d_y - T_y n \\ u_p &= -KS_y d_y - KS_y n \end{aligned} \tag{3.26}$$

The problem given in figure 3.3 can be rewritten in an $H\infty$ problem. Indeed, considering the general control configuration $\rho(s)$ of the plant model $G(s)$, the $H\infty$ control problem **??** **??** consists in finding $K(s)$ such that the closed-loop system is stable and :

$$\left\| \begin{matrix} W_y S_y & W_y T_y \\ W_u K S_y & W_u K S_y \end{matrix} \right\|_\infty \leq \gamma \tag{3.27}$$

This problem is a mixed sensitivity problem. It allows one to tackle the performances objectives by a frequency analysis of the sensitivity functions. So the disturbance rejection d_y impels the sensitivity functions S_y and KS_y to be small. And for a good rejection of the measurement noise (n), the functions T_y and KS_y must be small. And if the aim is for the output (y) to track the reference (r) the function T_y must be unitary. So these goals have to be achieved for different frequency ranges.

3.3 LMI based Hinf Control Suspensions Car

A linear matrix inequality (LMI) is an affine matrix-valued function,

$$f(x) = F_0 + \sum_{i=1}^{m} x_i F_i > 0S \tag{3.28}$$

where $x \in \mathbb{R}^m$ are called the decision variables and $F_i = F_i^T \in \mathbb{R}^{nn}$ are symmetric matrices.

A very important aspect of the LMI is that it defines a *convex set*. To see this, let x_1 and x_2 be two solutions to an LMI problem, i.e. $F(x_1) > 0$ and $F(x_2) > 0$. Then also any convex combination $x = (1 - \lambda)x_1 + \lambda x_2$, with $\lambda \in [0,\ 1]$ solves the LMI:

$$F(x) = F((1 - \lambda)x_1 + \lambda x_2) = (1 - \lambda)F(x_1) + \lambda F(x_2) > 0 \tag{3.29}$$

Recently, efficient numerical methods have been developed. The most efficient algorithms for solving LMI problems are based on interior point methods. These methods are iterative and each iteration includes a least squares minimization problem.

3.3.1 Example Linear Matrix Inequality

Most LMIs are not formulated in the standard form (1) but they can be rewritten as is shown in this example. Let us consider the following Lyapunov problem:

$$\begin{cases} P = P^T > 0 \\ A^T P + PA < 0 \end{cases}$$

Note that P enters linearly in both inequalities. To show how to rewrite this into the standard LMI form, we assume that $P \in \mathbb{R}^{2x2}$. Parametrize P as a linear function in x:

$$P(x) = x_1 \begin{bmatrix} 1 & 0 \\ 0 & 0 \end{bmatrix} + x_2 \begin{bmatrix} 0 & 1 \\ 1 & 0 \end{bmatrix} + x_3 \begin{bmatrix} 0 & 0 \\ 0 & 1 \end{bmatrix} = x_1 P_1 + x_2 P_2 + x_3 P_3.$$

Then $F(x) = diag[P(x), -A^T P(x) - P(x)A]$, or

$$F(x) = x_1 \begin{bmatrix} P_1 & 0 \\ 0 & -A^T P_1 - P_1 A \end{bmatrix} + x_2 \begin{bmatrix} P_2 & 0 \\ 0 & -A^T P_2 - P_2 A \end{bmatrix} + x_3 \begin{bmatrix} P_3 & 0 \\ 0 & -A^T P_3 - P_3 A \end{bmatrix}.$$

which is in the form (1) with $F(0) = 0$. In this case, three decision variables are needed. In general we need $n(n+1)/2$ decision variables for symmetric matrices and n^2 for full square matrices of size nn

3.3.2 Some Standard LMI Problems

Some standard LMI problems are listed in [BGFB94]. The most important ones are:

LMIP

The LMI problem is to find a feasible x such that $F(x) > 0$ or to determine if the LMI is infeasible.

As an example of an LMIP we take the problem in example 1.1 of finding a Lyapunov matrix

$$A^T P + PA < 0. \tag{3.30}$$

EVP/PDP

The eigenvalue problem(EVP) is to minimize the maximum eigenvalue of a matrix $A(x)$ that depends affinely on a variable subject to an LMI constraint. That is:

$$\min_{\lambda,x}\{\lambda : \lambda I - A(x) > 0, B(x) > 0\}. \tag{3.31}$$

This is equivalent to minimizing a linear function of x subject to an LMI constraint:

$$\min_{x}\{c^T x : F(x) > 0\} \tag{3.32}$$

The latter formulation is called positive definite programming (PDP) or, if the inequality is non strict, semi definite programming (SDP) [12].

As an example of an PDP we consider the bounded real lemma (lemma 2), which determines the $H\infty$ norm of a system $G(s) = D + C(sI - A)^{-0}B$ by minimizing λ with respect to $P > 0$ subject to:

$$\begin{bmatrix} PA + A^T P & PB & C^T \\ B^T P & -\lambda I & D^T \\ C & D & -\lambda I \end{bmatrix} < 0$$

Note that the LMI problem, $F(x) > 0$ can be formulated as an EVP by:

$$\min_{\lambda,x}\{\lambda : F(x) + \lambda I > 0\} \leq 0, \tag{3.33}$$

for which a feasible point, (λ, x), can be easily found for any initial x by choosing λ sufficiently large.

GEVP

The generalized eigenvalue problem is to minimize the maximum generalized eigenvalue of a pair of matrices that depend affinely on a variable, subject to an LMI constraint. The general form of a GEVP is:

$$\min_{\lambda,x}\{\lambda : \lambda B(x)A(x) > 0, B(x) > 0, C(x) > 0\}. \tag{3.34}$$

where $A(x)$, $B(x)$ and $C(x)$ are symmetric matrices that depend affinely (linearly) on $x \in \mathbb{R}^m$.

As an example of a GEVP we take the problem of finding the upper bound ν of the complex μ value of a matrix M. This problem is solved by minimizing $\nu > 0$ (or equivalently ν^2) with respect to $P > 0$ subject to $M^*PM < \nu^2$ The GEVP problem is not convex but quasi-convex.

3.3.3 Problem LMI based Hinf Problem

Before introducing the main result of this thesis, which uses well known $H\infty$, let us first recall some basic facts on LMI based $H\infty$ problem resolution for suspensions systems, we can see that a $H\infty$ controller is defined by:

$$S : \begin{bmatrix} \dot{x}_c \\ u \end{bmatrix} = \begin{bmatrix} A_c & B_c \\ C_C & D_C \end{bmatrix} \begin{bmatrix} x_c \\ y \end{bmatrix}$$

where x_c, y and u are the state, the control input and output, respectively, of the controller.

$A_c \in R^{n\times n}$, $B_c \in R^{n\times n_y}$, $C_c \in R^{n_u\times n}$, $D_c \in R^{n_u\times n_y}$

To make the LMI problem, we must do the following positions. Let k be the size of the controller:

$$P = \begin{bmatrix} X & N \\ N^T & F \end{bmatrix} \in R^{n+k\times n+k}$$

$$P^{-1} = \begin{bmatrix} Y & M \\ N^T & Z \end{bmatrix} \in R^{n+k\times n+k}$$

with: $X = X' \in R^{(n)\times(n)}, Y = Y' \in R^{(n)\times(n)}, N \in R^{(n)\times(k)}, M \in R^{n\times k}$

Of course $PP^{-1} = I$, but if this is true, then surely we can write:

$$P = \begin{bmatrix} X \\ M^T \end{bmatrix} = \begin{bmatrix} I_n \\ 0 \end{bmatrix}$$

Now if we introduce the following matrices:

$$\pi_y = \begin{bmatrix} Y & I_n \\ M^T & 0 \end{bmatrix}$$

$$\pi_x = \begin{bmatrix} I_n & X \\ 0 & N^T \end{bmatrix}$$

We can certainly write that:

$P\pi_y = \pi_x$

Going to apply them, we recall the following well-known results:

$R_1 = \pi_y^T P A_{cl} \pi_y = \pi_x^T A_{cl} \pi_y =$

$$= \begin{bmatrix} AY + B_1\hat{C}_K & A + B_1\hat{D}_k C \\ \hat{A}_k & XA + \hat{B}_k C \end{bmatrix}$$

$R_2 = \pi_y^T P \pi_y = \pi_x^T \pi_y =$

$$= \begin{bmatrix} Y & I \\ I & X \end{bmatrix}$$

$R_3 = \pi_y^T P B_{cl} = \pi_x^T B_{cl} =$

$$= \begin{bmatrix} B_2 + B\hat{D}_k D \\ XB_2 + \hat{B}\hat{B}_k D \end{bmatrix}$$

$R_{4,i} = \overline{C}_i \pi_y =$

$$= \begin{bmatrix} C_i Y + D_{i,2}\hat{C}_k \\ C_i + D_{i2}\hat{D}_k C \end{bmatrix}^T$$

Note that each of these is a combination of affine matrices where the auxiliary variables are:

$$\begin{cases} \widetilde{A} = NA_kM^T + NB_kCY + XBC_kM^T + \\ \quad X(A + BD_kC)Y \\ \widetilde{B} = NB_k + XBD_k \\ \widetilde{C} = C_kM^T + D_kCY \\ \widetilde{D} = D_k \end{cases}$$

Then, the H-inf control problem can be formulated as:

$$\left[\begin{array}{c|c|c} \pi_y A_{cl}^T P_\infty \pi_y + \pi_y^T P_\infty A_{cl} \pi_y & \pi_y P_\infty B_{cl} & \pi_y^T \overline{C}_1^T \\ \hline * & -\gamma_\infty I & \overline{D}_1^T \\ \hline * & * & -\gamma_\infty I \end{array}\right] < 0$$

from that:

$$\left[\begin{array}{c|c|c} R_1^T + R_1 & R_3 & R_{4,1} \\ \hline * & -\gamma_\infty I & \overline{D}_1^T \\ \hline * & * & -\gamma_\infty I \end{array}\right] < 0$$

Observe that the controller has to reach these objectives for the whole set of varying parameters.

Chapter 4

Simulations Result

The performance of the H_∞ control approach has been demonstrated through two suspension models, the the Half-car model the first and the Quarter-car model the second. In the sequel, the "active" and "passive" terms represent respectively the closed-loop $(--)$ case and the open-loop $(-.)$ case. Morevoer, in this chapter we will illustrate the results of simulation on simple Quarte-Car model, Simple Half-Car Model and Half-Car Model with Passenger. With QCTF we means the *Quarter-Car Transfer Functions* and with HCTF the *Half-Car Transfer Functions*.

4.1 Results of simple car model

4.1.1 Functions of Weight

Consider the weights $W_z$and W_n, selected according to the specifications imposed at the beginning. Since the controlled output is $z = [Z_s \ Z_u \ \ddot{Z}_s; u]$, the matrix $W_z$is chosen in this way:

$$W_z = diag(W_{zs}, W_{zu}, W_{zs2}, W_u)$$

The functions $W_{zs}and W_{zu}$ were chosen to improve performance solely on the sen-

sitivity the human body. Then, the transfer function between Z_r and Z_s is weighted between 1 and 10Hz while the one between Z_r and Z_u is weighted more between 8 and 14Hz. Both weighing functions $W_{zs} and W_{zu}$ are second order and are chosen so that their gains decrease quickly after 10Hz and 14Hz respectively. Figure 4.1 shows the frequency response of the chosen weighting functions. Once synthesized the controller, the corresponding frequency responses of the transfer functions of closed-loop system will be limited respectively by γ/W_{zs} and γ/W_{zu}

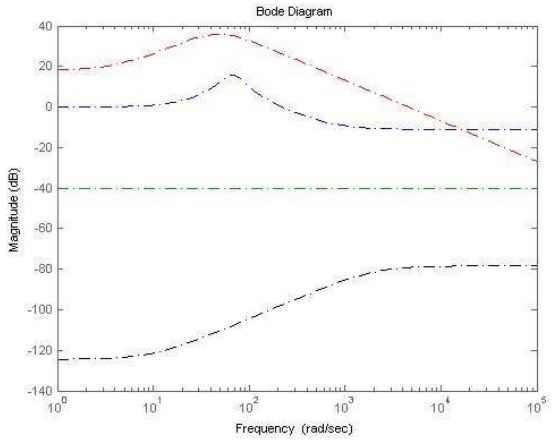

Figure 4.1 Functions of Weighing $(W_{zs}, W_{zu}, W_{zs2}, W_u)$

4.1.2 Results of simple car model

Function W_u is chosen so that the control signal u is limited to 10Hz. The functions W_{zs2} and W_n are chosen constants so as to not increase the order of the controller. Hereafter are reported the results of simulations, see Figures 4.2 and 4.3.

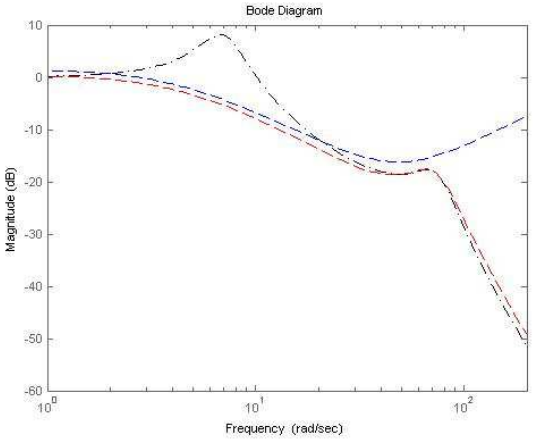

Figure 4.2 QCTF between road profiles y and chassis position x.

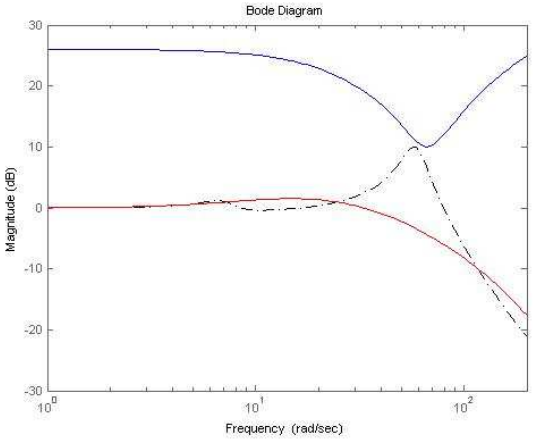

Figure 4.3 QCTF between road profiles y and chassis position $\ddot{x}$.

4.2 Results of Quarter-Car Model with Passenger

4.2.1 Frequency Domain

In this case the measure entering in controller are the acceleration of passengers $\ddot{x}_p$, while the unmeasured weighted controlled output are the chassis position x and the chassis acceleration $\ddot{x}$.

On Figure 4.4 and 4.5, the responses of the transfer functions from vertical road profiles y_i to vertical sprung mass position$x$ and acceleration $\ddot{x}$, respectively in passive and active cases, are compared.

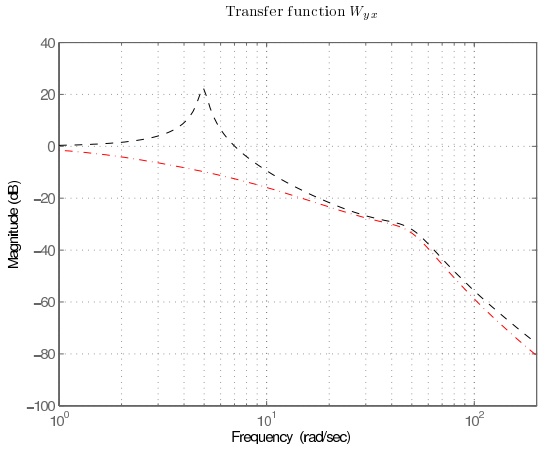

Figure 4.4 QCTF between road profiles y and chassis position x.

4.2.2 Time domain

In the time simulation for the quarter-vehicle the same road profile of the half-car case is used. The passenger comfort is more improved in this case, see fig 4.6.

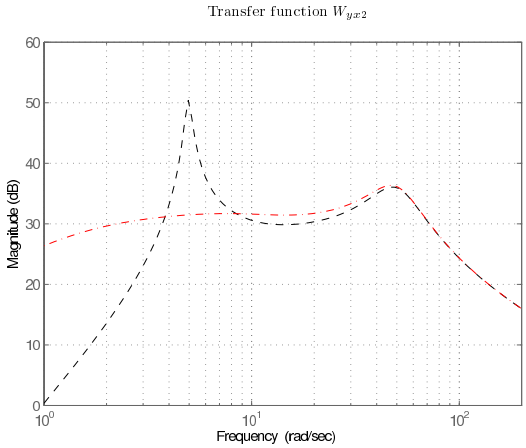

Figure 4.5 QCTF between road profiles y and chassis position $\ddot{x}$.

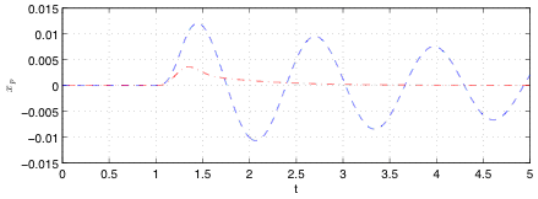

Figure 4.6 Quarter-car, Responses of passenger positions, in Time Domain

4.3 Results of Half-car model with passenger

4.3.1 Frequency Domain

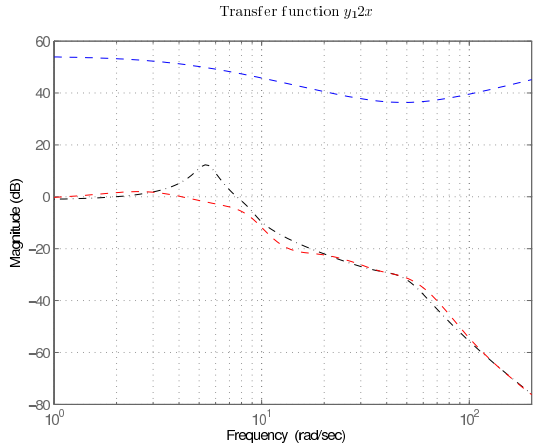

Figure 4.7 HCTF. between road profiles y_1 and chassis position x.

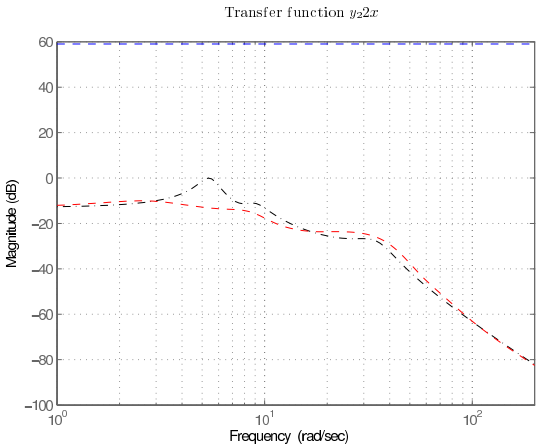

Figure 4.8 HCTF between road profiles y_2 and chassis position x.

In this case the measure entering in controller are the acceleration of passengers $\ddot{x}_{p1}$ and $\ddot{x}_{p2}$ while the unmeasured weighted controlled output are the chassis position x, the chassis acceleration $\ddot{x}$ and the pitch acceleration $\ddot{\theta}$.

On Figure 4.7 and Figure 4.8 we can see the responses of the transfer functions

from vertical road profiles y_1 and y_2 to vertical chassis mass position$x$ and acceleration $\ddot{x}$, respectively in passive and active cases.

On Figure 4.9 and Figure 4.10 we can note the responses of the transfer functions from vertical road profiles y_i to vertical acceleration $\ddot{x}$ in passive and active cases.

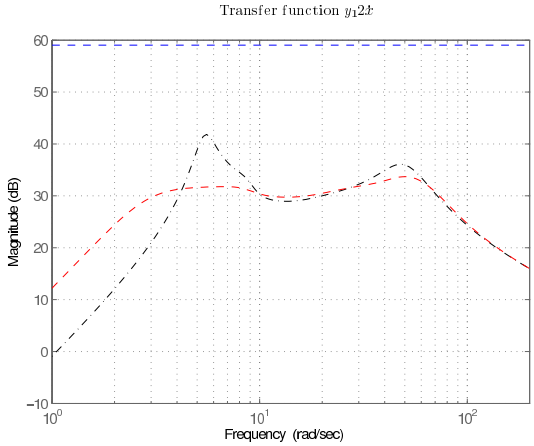

Figure 4.9 HCTF between road profiles y_1 and chassis acceleration $\ddot{x}$.

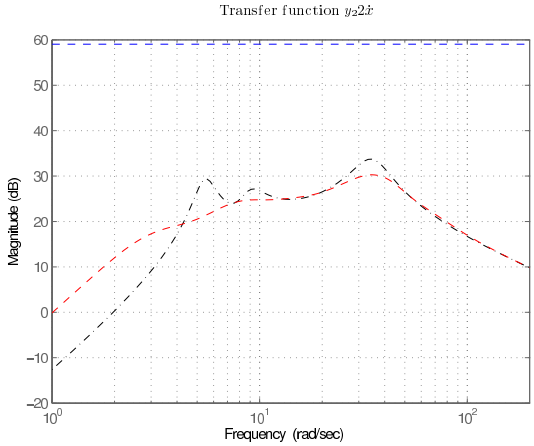

Figure 4.10 HCTF between road profiles y_2 and chassis acceleration $\ddot{x}$.

On Figure 4.11 and Figure 4.12 we can note that the comparisons between passive and active cases involve the response of transfer functions from vertical road profiles y_i to pitch acceleration $\ddot{\theta}$.

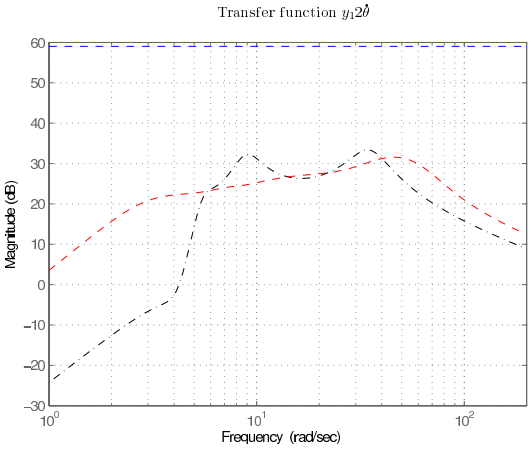

Figure 4.11 HCTF between road profiles y_1 and pitch acceleration $\ddot{\theta}$.

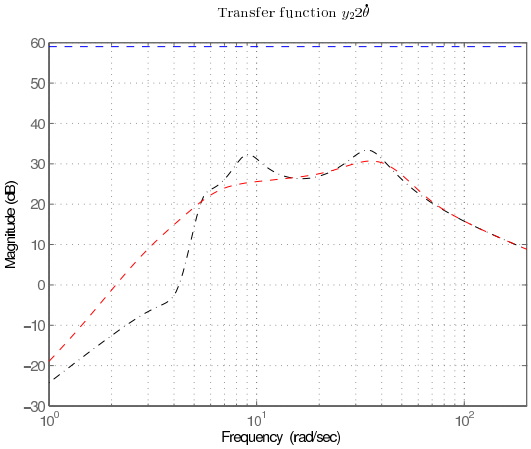

Figure 4.12 HCTF between road profiles y_2 and pitch acceleration $\ddot{\theta}$.

4.3.2 Time domain

In the time response, Figure 4.13 simulates half-vehicle running at speed of 70 km/h on road hump of 1 cm high and 10 cm long. By reducing the vertical chassis mass in the frequency range of human sensitivity, the passengers comfort is improved as expected.

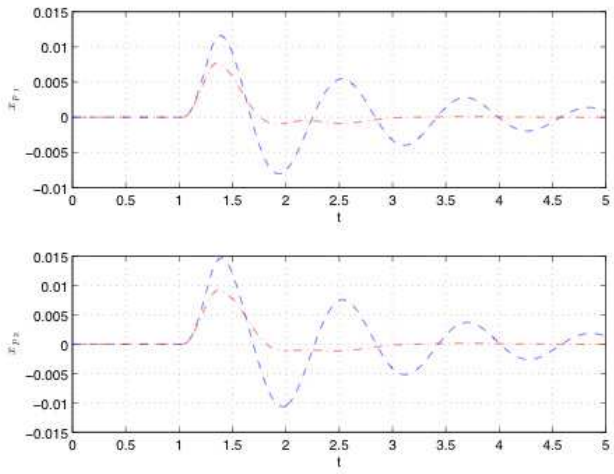

Figure 4.13 Half-car, Responses of passenger positions, in the time response

Chapter 5

Structural Control in Civil Engineering

Control studies in civil engineering can be divided into two categories: those which address serviceability issues and those whose main concern is safety. When serviceability is the main concern, control is used to reduce structural acceleration in order to increase occupant comfort during relatively mild wind or seismic excitations. However, for those controllers developed for stronger excitations, where occupant safety is the main concern, the goal is to improve structural response by reducing peak inter-story drift or by increasing energy dissipation.

5.1 Introduction

For structural control to gain viability in the earthquake engineering community, understanding the role of controllers within the context of performance-based engineering is of primary importance. Design of a structure controller system should involve a thorough understanding of how various types of controllers enhance struc-

tural performance, such that the most effective type of controller is selected for the given structure and seismic hazard. Controllers may be passive, requiring no external energy source, or active, requiring an external power source. Application of certain passive systems, including base isolation and viscous dampers, have become more common, leading to a reasonable understanding of how such systems reduce the dynamic behaviour of structures. However, few full-scale applications of active controllers exist and their assessment, either for structural performance or reduced-order controller implementation is less studied.

In this chapter, an introduction to structural control for buildings is presented. First, an overview of the types of energy dissipation system, that is passive, active or semi-active, is presented in a general sense. Then, topics in modelling active and semi-active control are discussed with emphasis on their mathematical models, control interaction, and control techniques applied to vibration mitigation in civil structures. Finally, a family of benchmark problems is introduced to illustrate the application of the model and controller reduction schemes described in the previous chapters.

5.2 Classification of Building Control

Structural control systems can be grouped into four broad areas [CSR05] based on the energy requirements of the control systems and the presence of sensors and the type of control algorithms:Base Isolation or Passive Control, Active Control, Semi-Active Control, and Hybrid Control. Base isolation can be considered the most widely-used control in building applications. The basic configuration of those systems is shown schematically in Figure 5.1 and their description is given below.

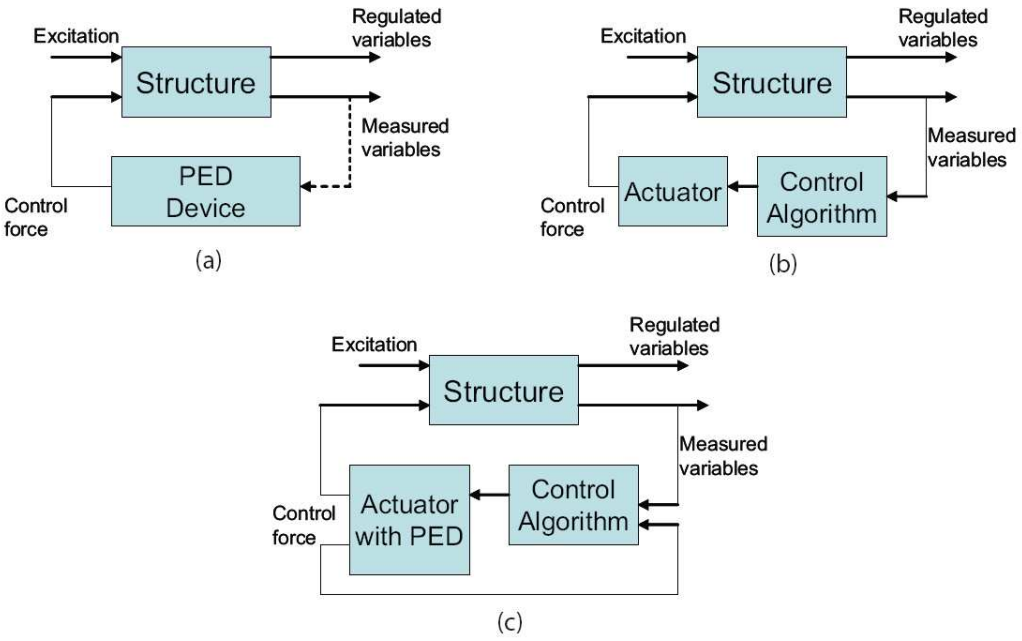

Figure 5.1 Passive *a*, Active *b*, and Semi-Active *c*

5.2.1 Passive Control

Passive control systems do not require external forces. The forces applied to the structural system are functions of the response to the excitation. By simply increasing the dissipated energy capacity of the structure through the use of special damper devices and materials, vibration mitigation can be accomplished.

Passive control may depend on the initial design of the structure, on the addition of viscoelastic material to the structure, on the use of impact dampers, or on the use of tuned mass dampers [HBC+97]. Initial design may use a tapered distribution of mass and stiffness, or use techniques of base isolation, where the lowest floor is deliberately made very flexible, thereby reducing the transmission of forces into the upper stories. Such schemes can be fairly successful in achieving their objectives. Though seldom as effective or hybrid control, passive control has four main advantages:

- it is usually relatively inexpensive;
- it consumes no external energy ;
- it is inherently stable;
- it works even during a major earthquake.

One of the most successful types of passive systems is called the base *Isolation System*, as shown in Figure 5.2. It is typically placed at the foundation of a structure. The isolation system introduces flexibility and energy absorption capabilities, thereby reducing the level of energy that can be transmitted to the structure. Another example of a passive control system employs passive supplemental damping devices, such as viscous dampers and tuned-mass dampers. Although passive control systems have reached a mature stage in technological development, they have inherent limitations. Usually, passive devices are optimally tuned to protect the structure from a particular dynamic loading or a particular mode of vibration (in general the first mode), and thus the performance of these devices is suboptimal for other loading scenarios and configurations.

5.2.2 Active Control

A logical extension of the passive control system is its enhancement with the addition of external inputs to the structure. Active control systems contain external powered actuators that apply forces in a pre-determined manner. They both add and dissipate energy in the structure. A computer-based control algorithm uses information from sensors to command the actuator system. The main advantage of active control systems is that they act simultaneously with the hazard excitation to provide enhanced structural behaviour for improved service and safety [CSR05]. The main drawback

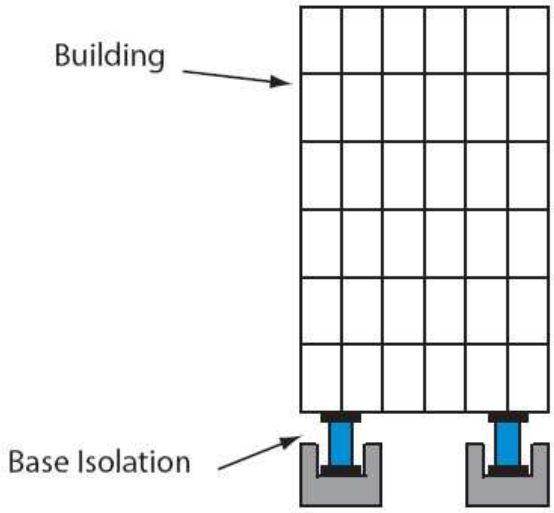

Figure 5.2 Base isolation schematic

of such systems stems from the fact that external power (actuators, motors) has to be added to the system, thus, increasing its complexity.

Active control systems can be implemented in several configurations like, *active bracing, active tendon*, and *active mass drivers*, among others. The differences are only on the type and direction of forces and torques applied to the structure. They all need an external power supply and a computer for the control implementation.

5.2.3 Semi-Active Control

A semi-active control system can be considered as a passive device whose properties can be actively controlled. For example, a fluid viscous damper whose damping constant can be controlled. These systems require power inputs that are significantly reduced from a fully active system. They can be implemented in a variety of schemes: variable-orifice dampers, variable-friction dampers, electro-rheological devices, and magneto-rheological devices.

The main advantages of semi-active control devices stem from the fact that they

operate on battery power and they do not destabilize the structure.

5.2.4 Hybrid Control

Lastly, by combining features of both passive and active control systems, a hybrid system can be used. A hybrid control may use active control to supplement and improve the performance of a passive control scheme. Alternatively, passive control may be added to an active control scheme to decrease its energy requirements. It should be noted in passing that the only essential difference between an active and a hybrid control scheme, in many cases, is the amount of external energy used to implement control.

5.3 Actuator Systems for Active and Semi-Active Building Control

Many different actuation systems have been implemented for applications in active and semi-active control of civil structures. The actuation schemes differ only in the type of force applied to the structure. In this dissertation, a few actuation systems are illustrated and only the active bracing system is used in the subsequent analysis.

5.3.1 Hydraulic Actuation and Active Bracing

The active bracing actuation system is usually placed across a single story level using a chevron or V-shape configuration. In large structures, they can span several story levels. There are other variations, such as X-braces. The system is comprised of a hydraulic actuator attached to the structure in order to create horizontal forces between floor diaphragm levels. For a hydraulic actuator system, the equation of

motion describing the fluid flow rate in an actuator can be linearised about the origin yielding [FSF93]

$$\dot{f}(t) = \frac{2\beta}{V}(Ak_q c(t) - K_c f(t) - A^2 \dot{x}_a(t)) \tag{5.1}$$

where c is the valve input, f is the force generated by the actuator, $A$is the cross-sectional area of the actuator, β is the bulk modulus of the fluid, V is the characteristic hydraulic fluid volume for the actuator, x_a is the actuator displacement, and (k_q, k_c), are system constants.

In general, the open-loop system in Eq. 5.1 is unstable. Closed-loop is essential for stabilization of the actuator. Also, the dynamics of the force applied by the actuator are dependent on the velocity response of the actuator, i.e., the feedback interaction path is intrinsic to the dynamical response of a hydraulic actuator. Incorporating unity gain displacement feedback into the hydraulic actuator model yields

$$\dot{f}(t) = \frac{2\beta}{V}(Ak_q \gamma(u(t) - x_a(t)) - K_c f(t) - A^2 \dot{x}_a(t)) \tag{5.2}$$

where u is the is the control command, and γ is a proportional feedback gain of the stabilizing controller for the actuator. Eq. 5.2 can be rewritten as

$$\dot{f}(t) = a_1 u(t) - a_1 x_a(t) - a_2 \dot{x}_a(t) - a_3 f(t) \tag{5.3}$$

where: $a_1 = \frac{2\beta k_q \gamma}{V}$, $a_2 = \frac{2\beta A^2}{V}$ and $a_3 = \frac{2\beta k_c}{V}$ we can write also the Eq. 5.3 in a state-space form, (it will be useful later for its implementation) as:

$$\dot{x}_a = A_a x_a + B_a u \tag{5.4}$$

$$y_a = C_a x_a + D_a u = f \tag{5.5}$$

let's take in the simple case when we have just a single actuator, it follows that

$$A_a = [-a_3], \quad B_a = [a_1 \ -a_1 \ -a_2], \quad C_a = 1, \quad D_a = [0 \quad 0 \quad 0]$$

5.3.2 Hydraulic Actuation and Active Tendons

The actuation system using an active tendon configuration is similar to the active bracing system, except that the forces generated by the hydraulic system are transmitted to the structure through a set of tendons or two pre tensioned cables spanning the inter-story space at angles in an X-pattern. A single degree-of-freedom structure is shown in Figure 5.3 The mathematical model of system is given by:

$$m\ddot{x}(t) + c\dot{x}(t) + kx(t) = -m\ddot{g}(t) + (4k_c cos\alpha)f(t) \tag{5.6}$$

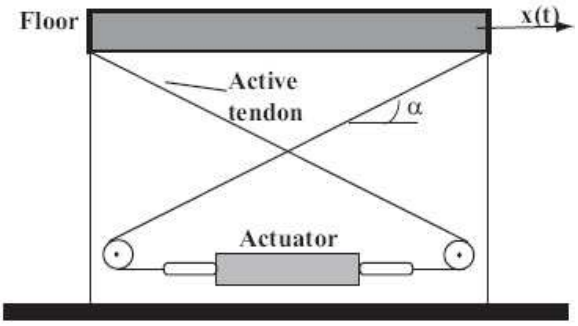

Figure 5.3 Hydraulic actuation and active tendon configuration.

where m, c, k are the mass, damping and stiffness of the structure, respectively, k_c is the tendon stiffness, α is the tendon inclination angle and f is the hydraulic actuator force as given by Eq. 5.2. The state-space equations follow the same ideas as for the active bracing system and will not be discussed here.

5.3.3 Hydraulic Actuation and the Active Mass Driver

The active mass driver actuation system is based on the base-excitation principle of structural systems [?] [Inm00], or what is called tuned mass damper. The idea is to incorporate a second spring-mass-damper into the system to change from a single-degree-of-freedom to a multi-degree-of-freedom in order to tune the motion of the original system. As an example, consider the spring-mass system shown in Figure 5.4 The equations of motion of the tuned-mass are given by

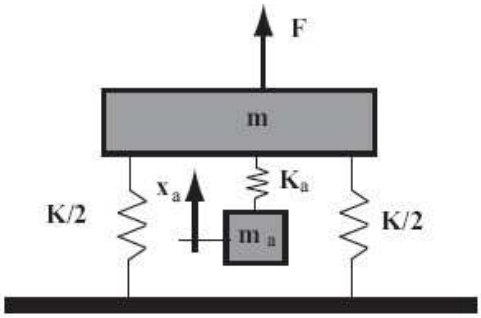

Figure 6.4: Tuned Mass-Damper

Figure 5.4 Tuned Mass-Damper.

One chooses the parameters of the added system (m_a, K_a) such that in the steady-state, the displacement of the original system is minimized. In this case, one can write the solution in the steady-state for the displacement of the structure and the added mass as

$$x_{ss}(t) = X sin\omega t \tag{5.7}$$

$$x_{a_{ss}}(t) = X_a sin\omega t \tag{5.8}$$

Substituting Eq. 5.7 and Eq. 5.7 into Eq. (dafare 110), yields

$$X = \frac{(k_a - m_a\omega^2)F_0}{(k + k_a - m\omega^2)(k_a - m_a\omega^2) - k_a^2} \tag{5.9}$$

$$X_a = \frac{(k_a F_0}{(k + k_a - m\omega^2)(k_a - m_a\omega^2) - k_a^2} \tag{5.10}$$

So, to minimize X, select ω according to

$$\omega^2 = \frac{k_a}{m_a} \tag{5.11}$$

One of the drawbacks of this approach is the lack of tuning in multiple frequencies, as shown by the tuning condition given in Eq. 5.11. For tuning the system at several frequencies, hydraulic actuators together with dampers can be added and feedback control techniques can be applied to enhance the performance of the entire system. In this case, a hybrid system is used and, hence, the system is called active-mass-driver.

5.4 Controllable Fluid Damper

In these devices some properties of their internal fluid can be modified by means of an electrical/magnetic field, resulting a modification in the quantity of force absorbed. The principal advantage of this type of devices is that the piston is the only moving part. Consequently, it can change rapidly from a state to another (linear viscous fluid to a semi-solid in milliseconds) when exposed to an electric/magnetic field. Two types of semi-active controllable fluid dampers are found: ***ER*** *Electro-rheological* and ***MR*** *Magneto-rheological* damper. Their difference is the type of fluid used: Magneto-rheological or Electro-rheological fluid.

5.4.1 Magneto-Rheological Damper Behaviour

The MR damper has become an alternative of ER damper. Its operation principle is similar to ER damper, except that the external signal applied is a magnetic field, which becomes the inside fluid from semi-solid to viscous state and it exhibits a viscoplastic behaviour similar to that of an ER fluid. MR devices with a high bandwidth can be constructed and controlled with low voltage (i.e. 12-24V) and low electrical currents about 1-2 amps. Batteries can supply this level of power. MR devices can operate at temperatures from -40C to 150C and slight variations occur in the yield stress. The transition velocity of both MR and ER devices is too fast (a few of milliseconds).

A MR damper model was developed in [SDSC97], where a simple mechanical model is used to describe its behaviour. Numerical examples and implementations to demonstrate the effectiveness of MR devices have been developed in [SDSC97]. These developments have demonstrated that MR dampers may be closed to the linear active control performance, while only a power fraction of that required by the active controller is enough. Lord Corporation designed and built a full-scale, 20-t MR damper, which could be the more biggest MR damper in structural control implementations. A schematic diagram of this device is shown in Figure 5.5.

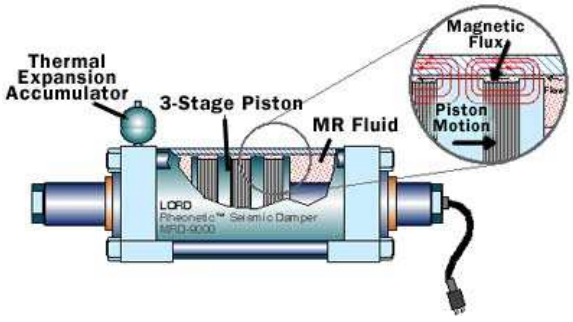

Figure 5.5 Magneto-rheological Dampers

Due to its promising characteristics, several studies have been undertaken in the past decade and several commercially available dampers have been developed. The mathematical model of an MR is very complex due to its non linear nature. Several models have been developed and tested in an experimental framework. One of the mechanical idealizations of the MR damped force that is numerically tractable uses the Bouc-Wen model for hysteretic systems. The most effective model for predicting the behaviour of an MR damper was proposed by Spencer [SDSC97], as shown in Figure 5.6 and can be mathematically modelled as follows:

$$f = \alpha z + c_0(\dot{x} - \dot{y}) + k_0(x - y) + k_1(x - x_0) = c_1 = c_1\dot{y} + k_1(x - x_0) \tag{5.12}$$

where the evolutionary variable z is governed by[45]

$$\dot{z} = -\lambda|\dot{x} - \dot{y}|z|z|^{n-1} - \beta(\dot{x} - \dot{y})|z|^n + A(\dot{x} - \dot{y}) \tag{5.13}$$

and

$$\dot{y} = \frac{1}{(c_0 + c_1)}[\alpha z + c_0\dot{x} + k_0(x - y)] \tag{5.14}$$

where F is the applied force of the damper, k_1 is the accumulator stiffness, c_0 is the viscous damping observed at larger velocities,c_1 is the damping introduced to model the non linear roll-off in the force-velocity at low velocities, k_0 is present to control the stiffness at higher velocities, and x_0 is the initial displacement of the spring k_1. The mathematical model can be determined by adjusting the parametersλ, β, A using system identification procedures.

To account for the dependence of the force on the voltage applied to the current

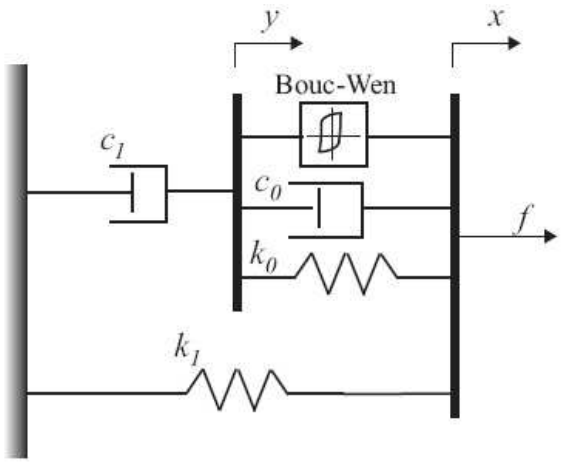

Figure 5.6 Schematic model of magneto-rheological dampers [SDSC97]

driver and the resulting magnetic current, one can use [SDSC97]

$$\alpha = \alpha(u) = \alpha_a u + \alpha_b u \tag{5.15}$$

$$c_1 = c_1(u) = c_{1a} u + c_{1b} u \tag{5.16}$$

$$c_0 = c_0(u) = c_{0a} u + c_{0b} u \tag{5.17}$$

where u is given as the output of a first-order filter given by

$$\dot{u} = \eta(u - \nu) \tag{5.18}$$

and ν is the commanded voltage sent to the current driver. Eq. 5.18 is necessary to model the dynamics involved in reaching rheological equilibrium and in driving the electromagnet in the MR damper.

In order to show the effectiveness of the proposed MR damper model, a simulation was performed in Matlab-Simulink using the same parameters as in [SDSC97] see Table 5.1 The MR block diagram is depicted in the Appendix A and the results due to a sinusoidal displacement input and several input voltages are given in Figure 5.7 and Figure 5.8.

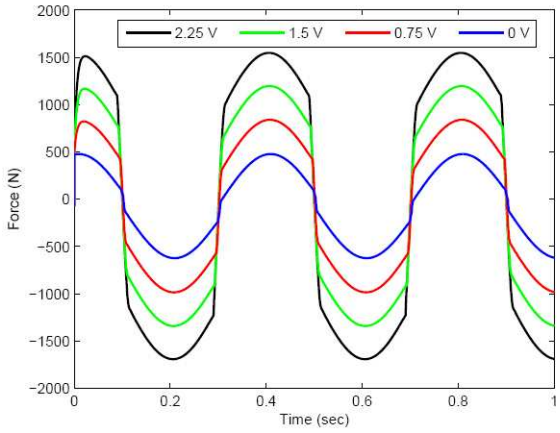

Figure 5.7 MR force due to a sinusoidal displacement and varying input voltages.

From Figure 5.7 and Figure 5.8, it can be seen that the force produced by the damper is not centred at zero. This effect is due to the presence of the accumulator in the MR damper. The enhancement on the MR output force can be observed in Figure 5.7, as voltage is increased from 0 V to 2.25 V . Also, the effects of changing the magnetic field are readily observed from Figure 5.8. At 0 V the MR damper function as a purely viscous device. As the voltage increases, the damper force also increase and produces behaviour associated with a plastic material in parallel with a viscous damper as shown by the hysteretic behaviour of the MR force and velocity. In the following sections, the effectiveness of the MR damper will be shown for seismic response reduction.

Table 5.1 Parameters for the MR Damper Model

Parameter	Value	Parameter	Value
c_{0a}	21.0 N sec/cm	α_a	140 N/cm
c_{0a}	3.50 N sec/cm V	α_b	695 N/cm V
k_0	46.9 N/cm	γ	363 cm^{-2}
c_{1a}	283 N sec/cm	β	363 cm^{-2}
c_{1a}	2.95 N sec/cm V	A	301
k_1	5.00 N/cm	n	2
x_0	14.3 cm	η	190 sec^{-1}

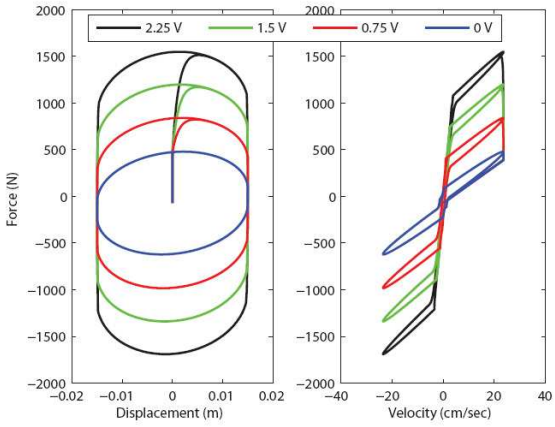

Figure 5.8 MR force due to a sinusoidal displacement and varying input voltages.

Chapter 6

Benchmark Civil Structural Control Problems

In general, civil structures are modelled as multi-story shear buildings [Paz97], that is, structures in which there is no rotation of a horizontal section at the level of the floors [Paz97] [Cra81]. In order to consider this simplification, several key assumptions have to be made:

1. The total mass of the structure is concentrated at the level of the floors;
2. The girders on the floor are infinitely rigid as compared to the columns;
3. The deformation of the structure is independent of the axial forces in the columns.

These assumptions transform the problem from a structure with an infinite number of degrees of freedom to a structure that has only as many degrees as it has lumped masses at the floor levels. Also, in some cases, the problem of a building comprised of several bays can be considered as a single bay, due to the rigidity of the floors. The mathematical model of a building subjected to an earthquake excitation is usually

considered as a response of a shear building to a base or foundation displacement. This can be accomplished if one considers the floor displacements relative to the base motion [Paz97] [Cra81]. Therefore, the equation of motion for the shear building can be written as

$$[M]\ddot{x}(t) + [D]\dot{x}(t) + [K]x(t) = B_s F(t) - [M]\Gamma\ddot{x}_g(t) \tag{6.1}$$

where $x(t)$ is the floor displacements relative to the base motion, M, D, K are, respectively, the mass, damping and stiffness of the building, B_s is a matrix of input selection, $F(t)$ is a matrix of external input forces from the control system, $\ddot{x}_g(t)$ is the earthquake excitation and finally,Γ is a matrix of ones on the respectively earthquake directions.

For control design problem, the building model can be rewritten in a state-space framework as

$$\begin{aligned}
\dot{x}(t) =& Ax(t) + BF(t) + E\ddot{x}_g(t) \\
y_m(t) =& C_m x(t) + D_m F(t) + F_m \ddot{x}_g(t) + v \\
z(t) =& C_z x(t) + D_z F(t) + F_z \ddot{x}_g(t) \\
y_c(t) =& C_c x(t) + D_c F(t) + F_c \ddot{x}_g(t)
\end{aligned} \tag{6.2}$$

where x is the state vector, y_m is the measured output vector, z is the regulated output vector, y_c is the feedback vector for the control devices, that is, the actuator connections due to the actuator-structure interactions [30], and v is the measurement noise. Also, the matrices D_m, D_z, D_c represent the contribution of the input vector on the respective output of the system (for instance, in the case of acceleration feedback), and the matrices F_m, F_z, F_c represent the contribution of the external disturbances (earthquake) to the respective output of the system. The state-space matrices are

$$A = \begin{bmatrix} 0 & I \\ -M^{-1}K & -M^{-1}D \end{bmatrix}, \quad B = \begin{bmatrix} 0 \\ M^{-1}B_s \end{bmatrix}; \quad E = \begin{bmatrix} 0 \\ -\Gamma \end{bmatrix} \tag{6.3}$$

For the case of position, velocity and acceleration measurements one can derive the following output matrices:

$$C_m = \begin{bmatrix} I & 0 \\ 0 & I \\ -M^{-1}K & -M^{-1}D \end{bmatrix}, \quad D_m = \begin{bmatrix} 0 \\ 0 \\ M^{-1}B_s \end{bmatrix} \tag{6.4}$$

Similar expressions can be derived for the regulated and the connections output matrices. In this dissertation, it will be assumed that

$$F_m = F_z = F_C = 0. \tag{6.5}$$

The state-space formulation can be modified in a way to include dynamics of the actuator and sensors (possibly a gain matrix). In this respect the actuators and sensor can be represented by their state-space form as

$$\sum_s : \quad y_{sensor}(t) = D_{sensor} Y_m(t) \tag{6.6}$$

$$\sum_a : \quad \begin{cases} \dot{x}_a(t) = A_a x_t + B_a \begin{bmatrix} u(t) \\ y_c(t) \end{bmatrix} \\ f_a(t) = C_a x_a(t) + D_a \begin{bmatrix} u(t) \\ y_c(t) \end{bmatrix} \end{cases} \tag{6.7}$$

The actuator input matrix can be partitioned according to the type of its inputs, i.e., $B_a = [B_{a1} \quad B_{a2}]$. In order to enhance performance of the control design, the actuator and structure models are lumped together forming only one design state-space system as

$$\begin{aligned} \dot{x}(d) =& A_d x + B_d F + E_d \ddot{x}_g \\ y_m =& C_{md} x + D_{md} F + F_{md} \ddot{x}_g + v \\ z_d =& C_{zd} x + D_{zd} F + F_{zd} \ddot{x}_g + v \end{aligned} \tag{6.8}$$

where

$$\begin{aligned} A_d =& \begin{bmatrix} A & BC_a \\ B_{a2}C_c & A + B_{a2}D_c C_a \end{bmatrix}, B_d = \begin{bmatrix} 0 \\ B_{a1} \end{bmatrix}, \\ E_d =& \begin{bmatrix} E_r \\ B_{a1}F_c \end{bmatrix} \\ C_{md} =& [C_m \quad D_m C_a], \quad C_{zd} = [C_z \quad |; D_z C_a] \\ D_{md} =& D_{zd} = 0, \quad F_{md} = F_m, \quad F_{md} = F_z \end{aligned} \tag{6.9}$$

6.1 Active Control Systems: The LQG Approach

Several control algorithms have been developed for the active control system, The most common approach for building control uses the LQG/H2 methods associated with linear controller. In this manner the control design problem can be formulated as follows:

Given the design model in state-space as in Eqs. (6.35), design a linear quadratic Gaussian (LQG) control algorithm for vibration reduction due to external inputs, such as earthquakes. The LQG solution minimizes the following performance index:

$$J = \lim_{\tau \to \infty} E \left[\int_0^\tau \{ z_d^T Q z_d + F_T R F \} \, dt \right] \tag{6.10}$$

where E is the expectation operator. An LQG controller is given by the following state-space equations:

$$\dot{x}_c(t) = (A_{d-B_dK-LC_{md}K})x_c(t) + Lu(t) \tag{6.11}$$

$$F(t) = -Kx_c(t) \tag{6.12}$$

where K, L are the regulator and estimator gains determined by the solution of two particular Riccati equations.

6.2 Semi-Active Control Systems: The Clipped Optimal Control Approach

Several control algorithms have been developed for semi-active systems. One algorithm that has been shown to be effective when used with MR dampers is the clipped-optimal control approach proposed by Dyke et al. The idea of the clipped-optimal control is to design a linear optimal controller $K_c(s)$, using a variety of synthesis methods (H2/LQG, for instance) to generate a vector of desired control forces f_c that would be achieved by the actuator if it could apply an active force to the system. Due to the dissipative nature of the semi-active device, this linear force cannot be achieved at all times. Thus, a logic has to be implemented in order to take into account the direction of the relative velocity of the control device.

The design of the linear optimal controller is based on the measured structural responses, i.e, y_m and the measured control force vector F applied to the structure, that is

$$f_c = \zeta^{-1}\{K_c(s)\zeta\{\begin{bmatrix} y_{md} \\ F \end{bmatrix}$$

where $\zeta\{.\}$ denotes the Laplace transform. In order to generate the desired optimal control force, a force feedback loop is added to induce the MR damper to generate approximately the desired optimal control force, such that the command voltage v is selected as follows.

When the MR damper provides the desired optimal force (i.e., $F = f_c$), the voltage applied to the damper should remain at the present level. If the magnitude of the force produced by the damper is smaller than the magnitude of the desired optimal force and both have the same sign, the voltage applied to the current driver is increased to the maximum level in order to increase the force produced by the damper to match the desired control force. Otherwise, the commanded voltage is set to zero. Mathematically, the above algorithm can be stated as

$$v = V_{max} H[(f_c - F)F] \tag{6.13}$$

where $H[]$ is the Heaviside step function and V_{max} is the voltage of the current driver associated with saturation of the magnetic field in the MR damper.

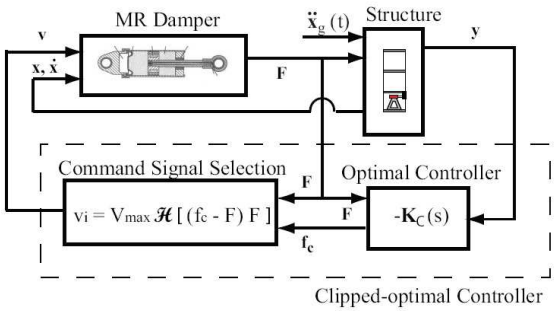

Figure 6.1 Clipped-Optimal Control Strategy

It should be pointed out that some modification of the LQG control law is necessary to take into account the clipped-optimal control strategy. Since the output of the controller is not any more a direct input to the plant, one needs to write

$$\dot{x}_c(t) = A_d x_C(t) + B_d F(t) + L[y_{md} - (C_{md} x_c(t) + D_{md} F(t))] \tag{6.14}$$

$$f_C(t) = -K x_C(t) \tag{6.15}$$

In this manner, the clipped-optimal controller becomes

$$\dot{x}_C = (A_d - LC_{md}) x_C(t) + [L \quad B_d - LD_{md}]... \tag{6.16}$$

$$f_C(t) = -K x_C(t) \tag{6.17}$$

6.3 Three-Story Building

A three story building is used to illustrate the active and semi-active controller implementations. The building is depicted in Figure 6.2. A hydraulic actuator (active bracing system) is placed at the first floor of the building and attached to the ground on the structure. For this system, the actuator displacement is equivalent to the displacement of the first floor. A position sensor is used to measure the displacement of the first floor and provide feedback for the control actuator. Also, accelerometers were placed on each floor for measurement of absolute accelerations. For comparison purposes a MR device is placed on the first floor using the same configuration as the active bracing system, and its controller is redesigned for the same building.

6.3.1 Active Bracing System

The mathematical model used here is taken from [20, 21]. The model consists of lumped masses at each floor with respective stiffness and damping effects. A hydraulic actuator is placed at the first floor. Numerically, the model is given by

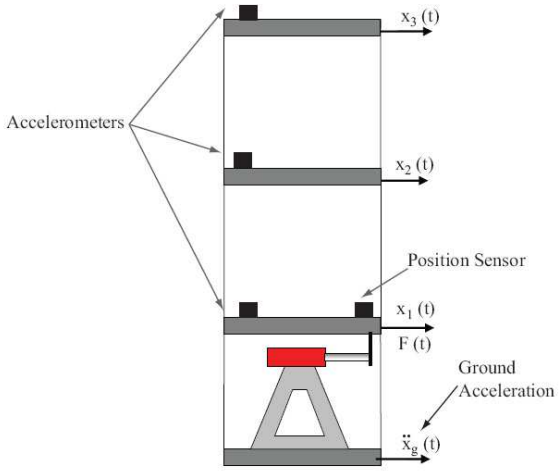

Figure 6.2 Three-story building schematic.

$$[M]\ddot{x}(t) + [C]\dot{x}(t) + [K]x(t) = B_s F(t) - [M]\Gamma\ddot{x}_g(t) \tag{6.18}$$

where

$$M = 125.2\begin{bmatrix} 5.6 & 0 & 0 \\ 0 & 5.6 & 0 \\ 0 & 0 & 5.6 \end{bmatrix}; \quad K = 175.2\begin{bmatrix} 15649 & -9370 & 2107 \\ -9370 & 17250 & -9274 \\ 2107 & -9274 & 7612 \end{bmatrix};$$

$$M = 125.2\begin{bmatrix} 2.185 & -0.327 & 0.352 \\ -0.327 & 2.608 & -0.015 \\ 0.352 & -0.015 & 2.497 \end{bmatrix}; \quad \Gamma = \begin{bmatrix} 1 \\ 1 \\ 1 \end{bmatrix}; \quad B_s = \begin{bmatrix} 1 \\ 1 \\ 1 \end{bmatrix}$$

with the following units: $M \rightarrow [kg]$,$K \rightarrow [N/m]$, $C \rightarrow [N*m/sec]$. The hydraulic actuator is modelled as in 5.3 and its parameters are given by :

$$a_1 = 6.08e5[kN/m*s]; \quad a_2 = 6.567e5[kN/m*s]; \quad a_3 = 29.6[1/s]$$

Using the acceleration of the all floors together with the displacement of the

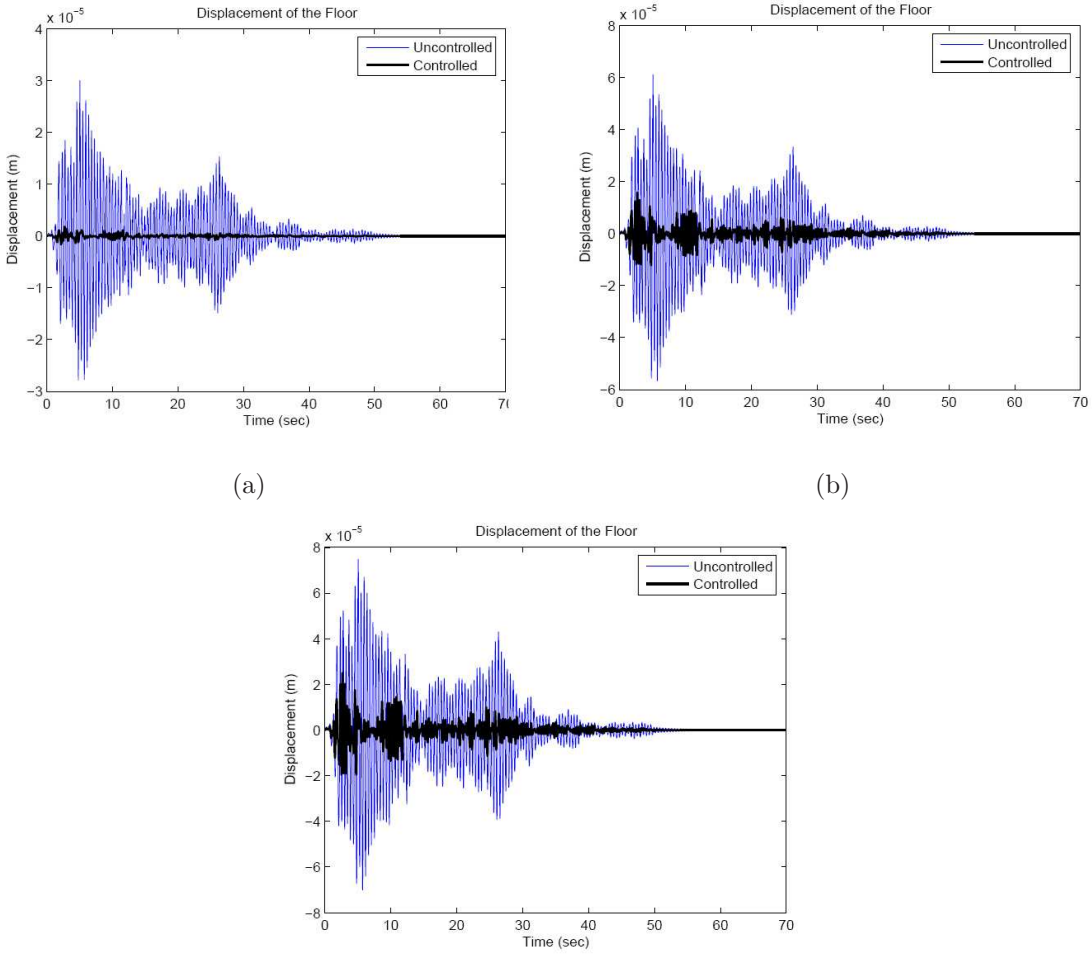

Figure 6.3 With a. b.: displacement of the (a) first, (b) second, and (c) third floors.

actuator as a regulated output vector, i.e, $z = [\ddot{x}_1 \ \ddot{x}_2 \ \ddot{x}_3 \ x_1$the results for an actual earthquake input (El Centro [ben]) is given in Figures 6.3, 6.4 and **??**.

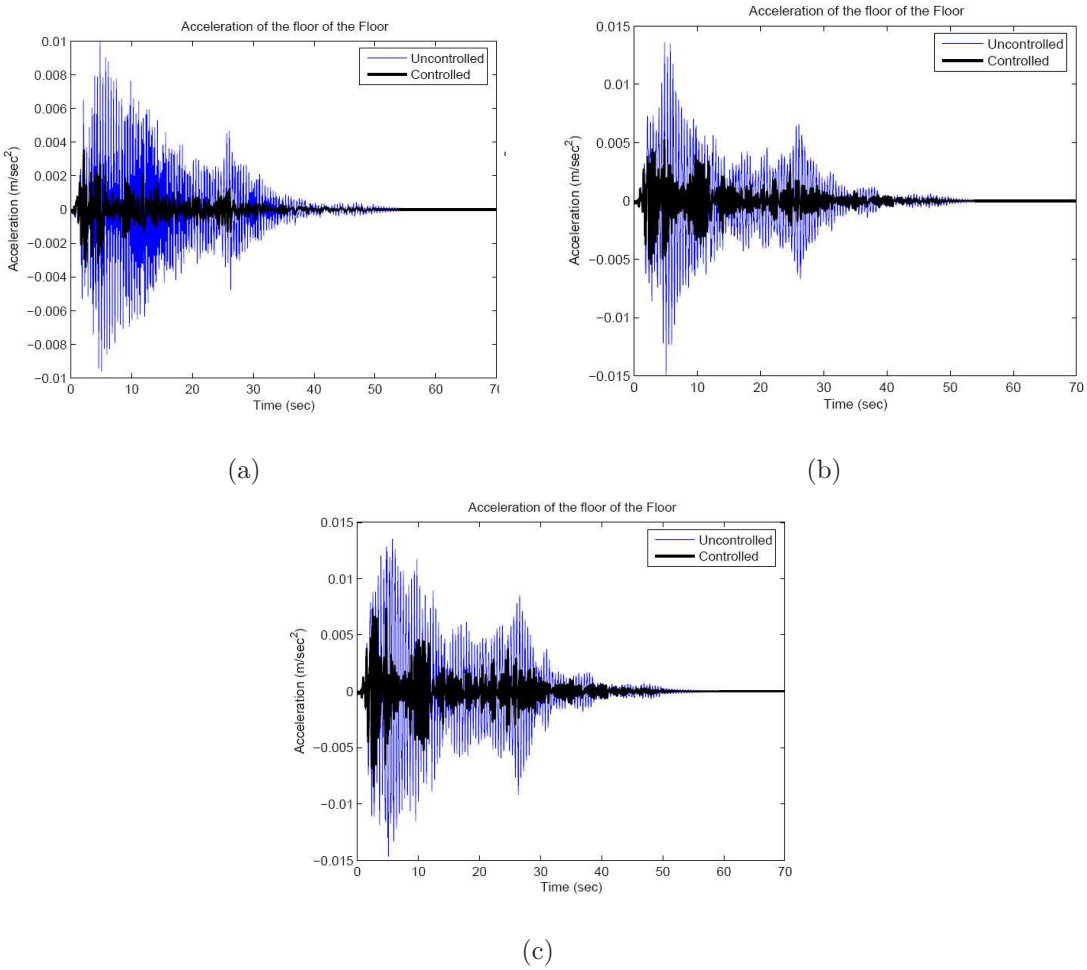

Figure 6.4 With a. b.: acceleration of the (a) first, (b) second, and (c) third floors.

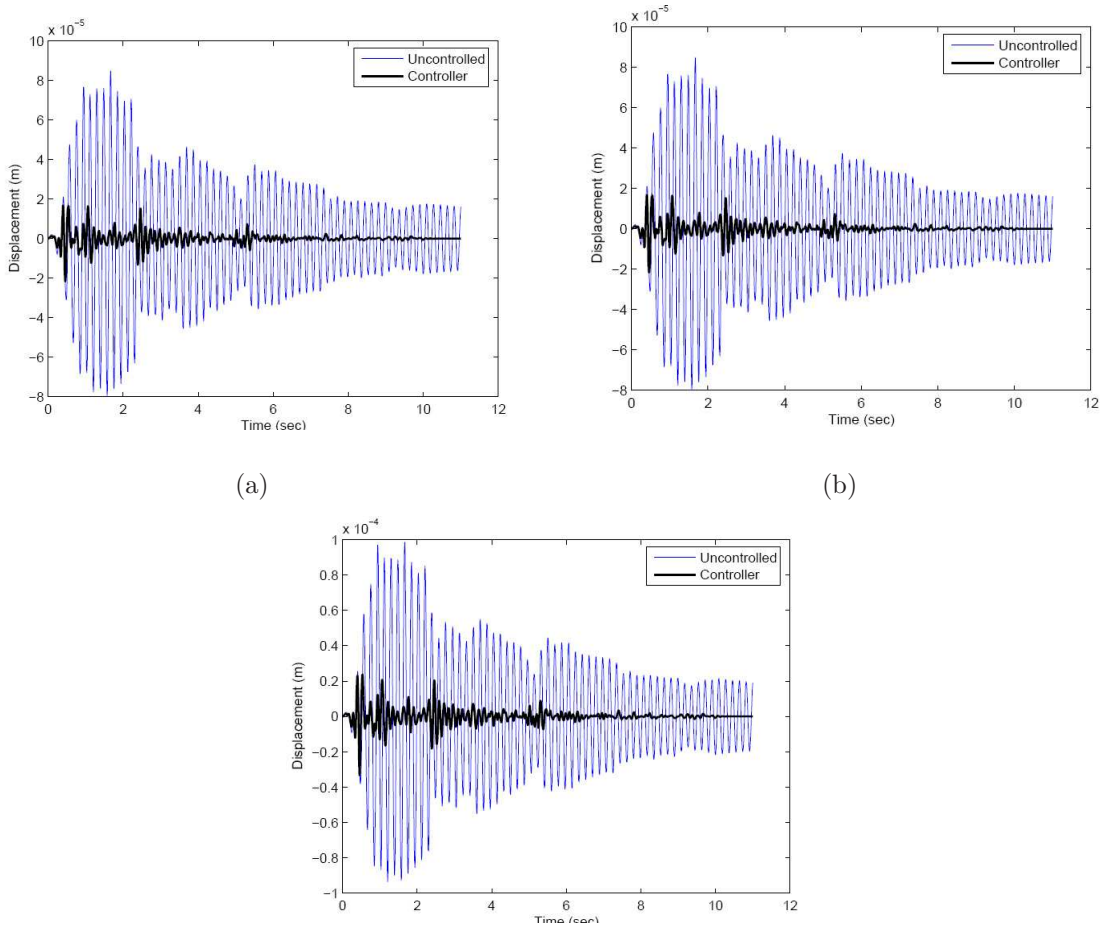

Figure 6.5 With MR: acceleration of the (a) first, (b) second, and (c) third floors.

Chapter 7

Conclusions and Future Work

In what follows some conclusions are provided for the two specific contributions of this thesis, namely the active control of automotive suspension systems and civil structures. Some indications on future studies are also discussed.

7.1 Conclusion

The purpose of this study was to develop an approach for the design of structural control systems with applications to automotive suspensions and civil structures based on the physical model of the systems. The effectiveness of the proposed control strategies have been demonstrated and evaluated through examples to car suspension systems by Lord Cooperation industry and to the benchmark smart base isolation problem by ASCE.

7.1.1 Automotive Suspension Systems

A new method of controlling active automotive suspension systems has been proposed here. The proposed method requires only the knowledge of the suspension stroke and

its velocity to generate the damping force. The suspension stroke and its velocity can be estimated from the acceleration of the vehicle body and wheels be means of a state observer. The controller design procedure is based on a frequency shaping approach and on H_∞ norm optimization. The aim of the active control was the attenuation of the oscillations in the prescribed frequency regions

A suspension model which uses two MR dampers for vibration suppression in the half-car model and one MR damper in the quarter-car model have been presented in this dissertation. The system has six degrees of freedom and two input forces provided by the MR actuators (in half-car model) and two degrees of freedom and one input force provide by MR actuator (in quarter-car model). An optimal controller is designed using acceleration feedback for the suspension system to suppress vibrations on the passenger seats. The simulation results indicate that the use of properly controlled MR actuators in the suspension of cars is a very promising idea.

7.1.2 Civil Structures

This thesis investigated active control of civil structures for natural hazard mitigation. The research has two components, the seismic protection of buildings and the mitigation of wind-induced vibration. Analytical and numerical methods are employed in the focused benchmark for illustrate the aim of the active control in civil structures engineering.

7.2 Future Research Directions

The goal of this dissertation was to provide an efficient controller design procedure well suited for the control of structural vibrations in automotive suspensions and civil structures. Some recommendations for future studies related to this work are

presented below:

7.2.1 Controllable MR Dampers

Magneto-rheological (MR) dampers have been successfully implemented in several fields of semi-active structural control: building control, car suspensions, bridge-control, and seat vibration, among others. Control strategies based on semi-active devices combine the best features of both passive and active control systems. In this dissertation, active control was considered for the controller vibrations reduction problem. It would therefore be interesting to apply the model and controller design procedures of this research to the case of semi-active control. Semi-active control strategies are based on nonlinear control methodologies. Thus, extensions to the problem to nonlinear control strategies should also be addressed.

The application of H_∞ control to Full-Car Suspension Model, so that to validate the real global behaviour, is a further point deserving investigations.

7.2.2 Large-scale Building Problems

In this dissertation, with the family of considered benchmark problems, reduced-order models were obtained for relatively small to medium systems. Even though the procedures presented for obtaining controllers can be used for large-scale systems, its effectiveness should be assessed. Building models comprised of fifty-thousand to several million states have already been obtained using finite element methods. Therefore, application of the passive-LQG design approach together with controller reduction methods should be investigated.

7.2.3 Nonlinear Building Models

Even though several important problems are still being investigated only for linear systems, the corresponding solutions are now quite effective. The next major challenge in the field of model and controller reduction is the application of such concepts to nonlinear systems. Several methods have been devised for model and controller reduction using the so-called proper orthogonal decomposition and its variants. However, there is not a general theory as in the linear case, and usually, the model reduction procedures are problem dependent. In the case of building models, large magnitude earthquakes can cause material yielding in the structural elements, and therefore, nonlinearities are present. The applications of linear model/controller reduction together with the nonlinear model reduction can be addressed using the third generation of benchmark problems.

Appendix A

Control Software

Control of suspension car and civil engineering structures with a digital computer or digital controller is becoming more and more common. Apart from the hardware equipment. the core of an active control system is the control software that generates the appropriate control command signals based on the response of the controlled many types of structures according to a proposed control algorithm, and sends out the remote control commands based on continuously monitored output of the controlled structure to trigger the operation of the active control force generation system. Although a number of control issues are theoretically solvable [CSR05], such as modelling errors, spillover effects, structural non linearities, limited number of sensors and controllers, discrete-time features, actuator dynamics. and time delay effect, the necessary knowledge about a practical control system is required to translate theoretical developments into practice. The control software, which includes the control signal generation, is intrinsically dependent on the control hardware and its implementation requires knowledge on real-time access to hardware and hardware functionality. To implement the proposed control algorithm on the control hardware, one needs to know how to gain access to the control hardware and how to control it through the

development of the microcode. The microcode is the code that is loaded permanently into a fixed location of the memory in a DCP/DSP. Microcode development for a digital control system is usually the most labor-intensive step in the design process. The control processor is almost always called upon to do more tasks than simply to implement the control equations and the microcode is usually supplied by someone other than the control engineer, which implies communication between engineers of different disciplines.

A.1 Practical Considerations

Although active control systems have been implemented to control suspension car, wind or earthquake induced vibration of buildings around the world and many others structures, there are still some practical and important issues to be addressed in order to ensure their performance under realistic conditions. They include time delay, structural non linearities, limited numbers of sensors and controllers, discrete- time features, and reliability. These issues are briefly described below.

A.1.1 Time Delay and Time Lag

In ideal situations, all operations in the control loop can he performed instantaneously. However, in reality. time is required to process measured information, to perform on-line computation, and to convert signals between analog and discrete values, These steps contribute to the time delays in the control feedback loop. Additionally, time lags due to actuator dynamics are often significant and will cause unsynchronized application of the control forces if they arc not appropriately accommodated. Improper consideration of these time lags will potentially cause instability in the system. Time lags can be accommodated by explicitly incorporating actuator dynamics into the

system model. Alternatively, time lags may also he modelled as a time delay and, as such, the designer may incorporate them into the discrete-time derivation and compensate for them in the optimization process. The second approach is followed herein.

A.1.2 Structural Nonlinearities

Most active control developments have been restricted to the consideration of linear structures. In reality. structures will inevitably become nonlinear at some point due to excessive excitation levels. Method of analysing and controlling structures in these situations must be developed, there are many advanced control algorithms that can deal with nonlinearity.

A.1.3 limited Number of Sensors and Controllers

From the viewpoint of practicality and economy, the number of sensors and controllers arc severely Limited for real structural applications. To be sure the development of control algorithms has been based on an arbitrary number of controllers and has included the case of an arbitrary number of sensors output feedback as long as the structural system is completely controllable and observable. it can be shown that, for structural systems with no repeated modal frequencies, they can be made controllable and observable by a single properly located sensor and a single properly located controller. It should be emphasized, however, that practical considerations and computational requirements often require more sensors and controllers to be used than these minimum numbers.

A.1.4 Discrete-Time Control Features

Another important consideration in real-time control implementation is the discrete-time nature in the application of a control algorithm. Continuous-time control algorithms can only be executed in discrete-time since a digital computer is usually used for on-line computation and control execution. As a consequence. response measurements are digitized as feedback signals and control forces are applied in the form of piecewise step functions through the use of analog-to-digital converters. Hence, they are not continuous functions as called for by continuous-time control algorithms.

A.1.5 Reliability

While reliability is of central importance in all areas of system analysis. design. and synthesis, it takes on an added dimension of complexity, both technologically and psychologically, when an active control system is relied upon to ensure safety a structure. First of all, when active control is only used to counter large environmental forces, it is likely that the control system will be infrequently activated. The reliability of a system operating largely in the standby mode and the related problems of maintenance and performance qualification become an important issue. Furthermore, active systems rely on external power sources which in turn, rely on all the support utility systems. These systems, unfortunately, are most vulnerable at the precise moment when they are most needed. The scope of the reliability problem is thus considerably enlarged if all possible ramifications are considered. Not to be minimized is the psychological side of the reliability problem. There may exist a significant psychological barrier on the part of the occupants of a structure in accepting the idea of an actively controlled structure, leading to perhaps perceived reliability-related concerns, The reliability problem can be addressed by identifying important factors influencing the

control system performance. Thus, a series of real-time tests must be performed to identify these important factors prior to final implementation. Again, the real-time simulator can help in this regard.

Appendix B

Hardware Description

The basic hardware function of the active loop in active, hybrid, and semi-active control systems contains similar components, and their generalized hardware function is represented by the block diagram shown in Figure B.1 In such a general configuration, the response of a structure under external excitation, the active device status, the remote control status, and the fail-safe monitoring status of the active control force generation system (ACFGS) (usually analog voltage signals) are measured and then sent to the custom-designed signal interface system (CDSIS) [CAS01]. The system information is collected and sent to the digital control system (DCS) via the data acquisition/conversion system (DACS) to perform major control processing. The required control forces calculated by the digital control system are used as analog command signals for the active control force generation system through the digital-to-analog converter. The analog command signals may have to be converted to the movements of the force generation device lithe displacement-controlled controllers are used in the ACFGS. Different kinds of signal formats may be required in coordination with the active/semi-active devices. Another remote control command is necessary to communicate between the analog control system and the digital control system to

perform system activation and software fail-safe monitoring functions. The common features of each item will be discussed in this chapter. Also, some specified hardware will be used as examples to illustrate the integrated hardware functions of a case study model.

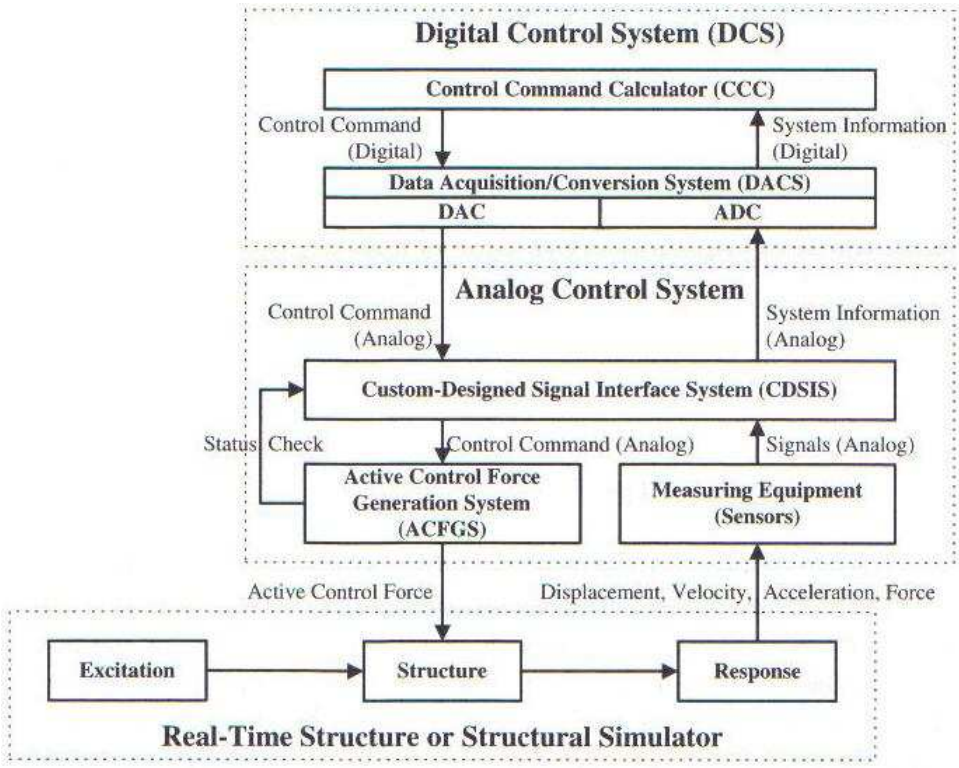

Figure B.1 General hardware function of the active control system. [CAS01]

B.1 Active Control Force Generation System

Active structural control may require the generation of control forces using high velocities and fast reaction times for which a new generation of actuators and control systems is required. Furthermore, appropriate control devices Thus be developed based not only on technological considerations hut also on economic, aesthetic, and

structural integration considerations. Due to its maturity and availability, an analog control system is usually implemented to perform this function. For an analog control system Figure B.2, the associated signals depend on the continuous-time variable where no signal sampling or data encoding is involved in the system. In order to generate the required control force, we must have access to the control console of the active device. In general, an active control force generation system contains three major parts as follows:

B.1.1 Control Device Power Supplier

This is the source of generating the required control forces and is dependent on the type of active device. In practical applications, electric power, compressed air, or hydraulic power is commonly used as the source.

B.1.2 Analog Control Console

This is the electronic portion of the control system and is used to drive the active devices and control the power supply. An analog controller also monitors and adjusts the function of the active device in order to generate correct active forces based on the required program command. The sources of program command will depend on the type of transducers employed on the active force generation device (AFGD). Either the force-controlled type or the displacement- controlled type is commonly used. The updated command signals are usually different from the outputs actually achieved at the beginning. By using a feedback control loop, the output measurements of system response are employed to modify the command signals so as to correct any output errors. The time lag of the achieved outputs from the command signals can be modelled as a time delay which is unavoidable and should be considered in the

theoretical development. To protect the whole system from damage in case the control system fails to perform properly or the performance error exceeds a preset limit, an analog fail-safe circuitry, which is capable of shutting down the control power. is required to monitor the response of the system. Due to various types of control mechanisms, the design of this fail-safe circuitry will depend on the specification of the active system. In practical applications, the operation of the force generation systcm is activated by the remote operation feature, which is provided by the digital control system under continuous monitoring of the response of the controlled structure and is triggered when it exceeds the preset level. A software shut-down fail-safe function embedded in the microcode inside the digital control system runs in parallel as a back-up. Thus, a certain type of communication between this analog control console and the digital controller has to be developed.

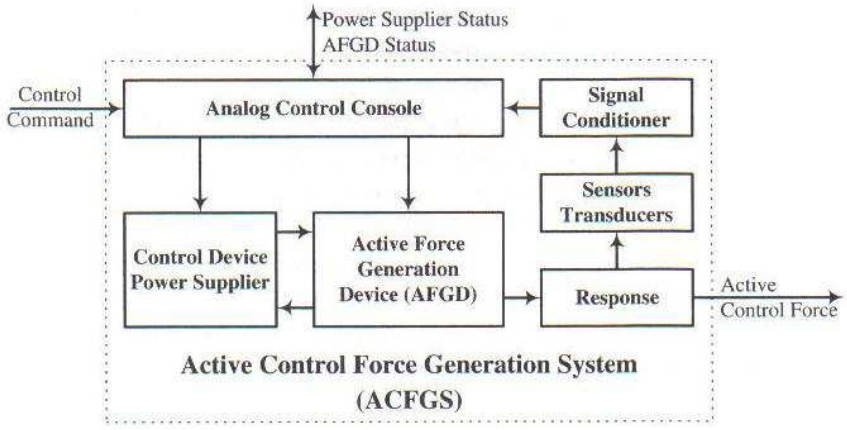

Figure B.2 Active control force generation system(ACFGS) [CAS01].

B.1.3 Active Force Generation device (AFGD)

The active force generation device is a combination of devices driven by either hydraulic, electric. or other power sources that mechanically drives a controlled system.

Factors such as power, motion resolution, repeatability, and an operation bandwidth requirement for a force generation system can differ significantly, depending on the particular control system. Proper selection of an active force generation device for a particular application is of the utmost importance in the instrumentation and design of a control system. Moreover, the actuatorstructure interaction (also known as the controlstructure interaction) is present in any mechanical control device. In order to include this interaction effect, response of the actuator can be explicitly modelled and then included in the model of the structural system ([SDSC97]).

Bibliography

[Ath03] M. Athans. The role and use of the stochastic linear-quadratic-gaussian problem in control system design. *Automatic Control, IEEE Transactions on*, 16(6):529–552, January 2003.

[ben] Vibrationdata. http://www.vibrationdata.com/elcentro.htm. el centro earthquake page. Technical report.

[BGFB94] S. Boyd, L. El Ghaoui, E. Feron, and V. Balakrishnan. *Linear Matrix Inequalities in Systems and Control Theory*. SIAM Studies in Applied Mathematics, 1994.

[CAS01] Steen T. Clausen, Palle Andersen, and Jakob Stoustrup. *Robust Control*. 2001.

[Cra81] Roy R. Craig. *Structural Dynamics: An Introduction to Computer Methods*. Wiley, August 1981. ISBN 0471044997.

[CSR05] S. Y. Chu, T. T. Soong, and A. M. Reinhorn. *Active, Hybrid, and Semiactive Structural Control: A Design and Implementation Handbook*. Wiley, August 2005. ISBN 0470013524.

[Dai90] R. Lane Dailey. Lecture notes for the workshop on h infinity and methods for robust control. May 1990.

[Dav75] Denny C. Davis. A radial-spring terrain-enveloping tire model. *Vehicle System Dynamics: International Journal of Vehicle Mechanics and Mobility*, 4(1):55–69, 1975.

[Duk00] Rao V. Dukkipati. *Vehicle Dynamics*. Narosa, 1 edition, October 2000. ISBN 084930976X.

[Fra87] B. A. Francis. *A Course in H-infinity Control Theory*. 1987.

[FSF93] M. Q. Feng, M. Shinozuka, and S. Fujii. Frictioncontrollable sliding isolated system. *g. Eng. Mech.*, 1993.

[Gil92] T. Gillispie. *Fundamental of Vehicle Dynamics*. 1992.

[GL] Michael Green and David J. N. Limebeer. *Linear Robust Control (Prentice Hall Information and System Sciences)*. Prentice Hall. ISBN 0131022784.

[Gob01] M. Gobbi. Analytical description and optimization of the dynamic behaviour of passively suspended road vehicles. *Journal of Sound and Vibration*, 245(3):457–481, August 2001.

[GSS+08] Emanuele Guglielmino, Tudor Sireteanu, Charles W. Stammers, Gheorghe Ghita, and Marius Giuclea. *Semi-active Suspension Control: Improved Vehicle Ride and Road Friendliness*. Springer, 1 edition, July 2008. ISBN 1848002300.

[HBC+97] G. W. Housner, L. A. Bergman, T. K. Caughey, A. G. Chassiakos, R. O. Claus, S. F. Masri, R. E. Skelton, T. T. Soong, B. F. Spencer, and J. T. P. Yao. Structural control: Past, present, and future. *Journal of Engineering Mechanics*, 123(9):897–971, 1997.

[Htt] Http://www. Lord mr solutions: The commercial leader in mr technology.

[Inm00] Daniel J. Inman. *Engineering Vibration, Second Edition*. Prentice Hall, 2 edition, August 2000. ISBN 013726142X.

[JSEG01] Zhenyu Jiang, Donald A. Streit, and Moustafa El-Gindy. Heavy vehicle ride comfort: literature survey. *International Journal of Heavy Vehicle Systems*, 8(3):258–284, January 2001.

[KZ06] Mansour A. Karkoub and Mohamed Zribi. Active/semi-active suspension control using magnetorheological actuators. *Intern. J. Syst. Sci.*, 37(1): 35–44, January 2006.

[LRG01] A. Liberzon, D. Rubinstein, and P. O. Gutman. Active suspension for single wheel station of off-road track vehicle. *International Journal of Robust and Nonlinear Control*, 11(10):977–999, 2001.

[MG00] N. J. Mansfield and M. J. Griffin. Non-linearities in apparent mass and transmissibility during exposure to whole-body vertical vibration. *Journal of Biomechanics*, pages 933–941, August 2000.

[Paz97] Mario Paz. *Structural Dynamics: Theory and Computation*. Chapman & Hall, 4th edition, July 1997. ISBN 0412074613.

[RL98] E. Reithmeier and G. Leitman. Robust control of seismic structures employing active. suspension elements. 1998.

[SDSC97] B. F. Spencer, S. J. Dyke, M. K. Sain, and J. D. Carlson. Phenomenological model for magnetorheological dampers. *Journal of Engineering Mechanics*, 123(3):230–238, 1997.

[SH86] R. S. Sharp and A. Hassan. The relative performance capabilities of passive, active and semi-active car suspension systems. 1986.

[TE98] Hamid D. Taghirad and E. Esmailzadeh. Automobile passenger comfort assured through lqg/lqr active suspension. *Journal of Vibration and Control*, 4(5):603–618, September 1998.

[Wei98] L. Wei. The prediciton of seat transmissibility from measures of seat impedance. *Journal of Sound and Vibration*, 214(1):121–137, July 1998.

[Wet97] H. L. Wettergren. On the behavior of material damping due to multi-frequency excitation. *Journal of Sound and Vibration*, pages 725–735, October 1997.

[WG98] L. Wei and M. J. Griffin. Mathematical models for the apparent mass of the seated human body exposed to vertical vibration. *Journal of Sound and Vibration*, pages 855–874, May 1998.

[Won08] J. Y. Wong. *Theory of Ground Vehicles*. Wiley, 4 edition, August 2008. ISBN 0470170387.

[YF00] Kazuo Yoshida and Tadahiro Fujio. Semi-active base isolation for a building structure. *International Journal of Computer Applications in Technology*, 13(1):52–58, January 2000.